

## Glasses and Aging: A Statistical Mechanics Perspective

LUDOVIC BERTHIER<sup>1</sup>, GIULIO BIROLI<sup>2</sup>

<sup>1</sup> Laboratoire des Colloïdes, Verres et Nanomatériaux, Université Montpellier II and CNRS, Montpellier, France

<sup>2</sup> Service de Physique Théorique Orme des Merisiers, CEA Saclay, Gif sur Yvette Cedex, France

### Article Outline

Glossary

Definition of the Subject

Phenomenology

Taxonomy of ‘Glasses’ in Science

Numerical Simulations

Dynamic Heterogeneity

Some Theory and Models

Aging and Off-equilibrium

Future Directions

Acknowledgements

Bibliography

### Glossary

In this preliminary section, a few concise definitions of the most important concepts discussed in this article are given.

**Glass transition** For molecular liquids, the glass transition denotes a crossover from a viscous liquid to an amorphous solid. Experimentally, the crossover takes place at the glass temperature,  $T_g$ , conventionally defined as the temperature where the liquid’s viscosity reaches the arbitrary value of  $10^{12}$  Pa.s. The glass transition more generally applies to many different condensed matter systems where a crossover or, less frequently, a true phase transition, takes place between an ergodic phase and a frozen, amorphous glassy phase.

**Aging** In the glass phase, disordered materials are characterized by relaxation times that exceed common observation timescales, so that a material quenched in its glass phase never reaches equilibrium (neither a metastable equilibrium). It exhibits instead an aging behaviour during which its physical properties keep evolving with time.

**Dynamic heterogeneity** Relaxation spectra of dynamical observables, e.g. the dynamical structure factor, are very broad in supercooled liquids. This is associated to a spatial distribution of timescales: at any given time, different regions in the liquid relax at different rates.

Since the supercooled liquid is ergodic, slow regions eventually become fast, and vice versa. Dynamic heterogeneity refers to the existence of these non-trivial spatio-temporal fluctuations in the local dynamical behaviour, a phenomenon observed in virtually all disordered systems with slow dynamics.

**Effective temperature** An aging material relaxes very slowly, trying (in vain) to reach its equilibrium state. During this process, the system probes states that do not correspond to thermodynamic equilibrium, so that its thermodynamic properties can not be rigorously defined. Any practical measurement of its temperature becomes a frequency-dependent operation. A ‘slow’ thermometer tuned to the relaxation timescale of the aging system measures an effective temperature corresponding to the ratio between spontaneous fluctuations (correlation) and linear response (susceptibility). This corresponds to a generalized form of the fluctuation-dissipation theorem for off-equilibrium materials.

**Frustration** Impossibility of simultaneously minimizing all the interaction terms in the energy function of the system. Frustration might arise from quenched disorder (as in the spin glass models), from competing interactions (as in geometrically frustrated magnets), or from competition between a ‘locally preferred order’, and global, e.g. geometric, constraints (as in hard spheres packing problems).

### Definition of the Subject

Glasses belong to a well-known state of matter: we easily design glasses with desired mechanical or optical properties on an industrial scale, they are widely present in our daily life. Yet, a deep microscopic understanding of the glassy state of matter remains a challenge for condensed matter physicists [6,67]. Glasses share similarities with crystalline solids (they are both mechanically rigid), but also with liquids (they both have similar disordered structures at the molecular level). It is mainly this mixed character that makes them fascinating even to non-scientists.

A glass can be obtained by cooling the temperature of a liquid below its glass temperature,  $T_g$ . The quench must be fast enough that the more standard first order phase transition towards the crystalline phase is avoided. The glass ‘transition’ is not a thermodynamic transition at all, since  $T_g$  is only empirically defined as the temperature below which the material has become too viscous to flow on a ‘reasonable’ timescale (and it is hard to define the word ‘reasonable’ in any reasonable manner). There-

Please note that the pagination is not final; in the print version an entry will in general not start on a new page.

92 fore,  $T_g$  does not play a fundamental role, as a phase tran- 143  
 93 sition temperature would. It is simply the temperature be- 144  
 94 low which the material looks solid. When quenched in 145  
 95 the glass phase below  $T_g$ , liquids slowly evolve towards 146  
 96 an equilibrium state they cannot reach on experimental 147  
 97 timescales. Physical properties are then found to evolve 148  
 98 slowly with time in far from equilibrium states, a process 149  
 99 known as ‘aging’ [152]. 150

100 Describing theoretically and quantifying experimen- 151  
 101 tally the physical mechanisms responsible for the viscos- 152  
 102 ity increase of liquids approaching the glass transition 153  
 103 and for aging phenomena below the glass transition cer- 154  
 104 tainly stand as central open challenges in condensed mat- 155  
 105 ter physics. Since statistical mechanics aims at understand- 156  
 106 ing the collective behaviour of large assemblies of interact- 157  
 107 ing objects, it comes as no surprise that it is a central tool in 158  
 108 that field. We shall therefore summarize the understand- 159  
 109 ing gained from statistical mechanics perspectives into the 160  
 110 problem of glasses and aging. 161

111 The subject has quite broad implications. A material 162  
 112 is said to be ‘glassy’ when its typical relaxation timescale 163  
 113 becomes of the order of, and often much larger than, the 164  
 114 typical duration of an experiment or a numerical simula- 165  
 115 tion. With this generic definition, a large number of sys- 166  
 116 tems can be considered as glassy materials [173]. One can 167  
 117 be interested in the physics of liquids (window glasses are 168  
 118 then the archetype), in ‘hard’ condensed matter (for in- 169  
 119 stance type II superconductors in the presence of disorder 170  
 120 such as high- $T_c$  superconducting materials), charge den- 171  
 121 sity waves or spin glasses, ‘soft’ condensed matter with nu- 172  
 122 merous complex fluids such as colloidal assemblies, emul- 173  
 123 sions, foams, but also granular materials, proteins, etc. All 174  
 124 these materials exhibit, in some part of their phase dia- 175  
 125 grams, some sort of glassy dynamics characterized by 176  
 126 a very rich phenomenology with effects such as aging, hys- 177  
 127 teresis, creep, memory, effective temperatures, rejuvena- 178  
 128 tion, dynamic heterogeneity, non-linear response, etc. 179

130 This long list explains why this area of research has re- 180  
 131 ceived increasing attention from physicists in the last two 181  
 132 decades. ‘Glassy’ topics now go much beyond the physics 182  
 133 of simple liquids (glass transition physics) and models 183  
 134 and concepts developed for one system often find appli- 184  
 135 cations elsewhere in physics, from algorithmics to bio- 185  
 136 physics [55]. Motivations to study glassy materials are nu- 186  
 137 merous. Glassy materials are everywhere around us and 187  
 138 therefore obviously attract interest beyond academic re- 188  
 139 search. At the same time, the glass conundrum provides 189  
 140 theoretical physicists with deep fundamental questions 190  
 141 since classical tools are sometimes not sufficient to prop- 191  
 142 erly account for the glass state. Moreover, simulating in the computer the dynamics of microscopically realistic mate-

rial on timescales that are experimentally relevant is not an 143  
 easy task, even with modern computers. 144

145 Studies on glassy materials constitute an exciting re- 146  
 147 search area where experiments, simulations and theoret- 148  
 149 ical calculations can meet, where both applied and fun- 149  
 150 damental problems are considered. How can one ob- 150  
 151 serve, understand, and theoretically describe the rich phe- 151  
 152 nomenology of glassy materials? What are the fundamen- 152  
 153 tal quantities and concepts that emerge from these de- 153  
 154 scriptions? 154

155 The outline of the article is as follows. In Sect. “Phen- 155  
 156 omenology” the phenomenology of glass-forming liquids 156  
 157 is discussed. In Sect. “Taxonomy of ‘Glasses’ in Science” 157  
 158 other type of glasses are described, in particular colloids 158  
 159 and granular materials. It is then described how computer 159  
 160 simulations have provided deep insights into the glass 160  
 161 problem in Sect. “Numerical Simulations”. The issue of 161  
 162 dynamic heterogeneity is tackled in Sect. “Dynamic Het- 162  
 163 erogeneity”. The main theoretical perspectives currently 163  
 164 available in the field are then summarized in Sect. “Some 164  
 165 Theory and Models”. Aging and off-equilibrium phenom- 165  
 166 ena occupy Sect. “Aging and Off-equilibrium”. Finally, is- 166  
 167 sues that seem important for future research are discussed 167  
 168 in Sect. “Future Directions”. 168

## 167 Phenomenology

### 168 Basic Facts

169 A vast majority of liquids (molecular liquids, polymeric 169  
 170 liquids, etc.) form a glass if cooled fast enough in order 170  
 171 to avoid the crystallisation transition [6]. Typical values of 171  
 172 cooling rate in laboratory experiments are 0.1–100 K/min. 172  
 173 The metastable phase reached in this way is called ‘super- 173  
 174 cooled phase’. In this regime the typical timescales increase 174  
 175 in a dramatic way and they end up to be many orders of 175  
 176 magnitudes larger than microscopic timescales at  $T_g$ , the 176  
 177 glass transition temperature. 177

178 For example, around the melting temperature  $T_m$ , the 178  
 179 typical timescale  $\tau_\alpha$  on which density fluctuations relax, 179  
 180 is of the order of  $\sqrt{ma^2/K_B T}$ , which corresponds to few 180  
 181 picoseconds ( $m$  is the molecular mass,  $T$  the tempera- 181  
 182 ture,  $K_B$  the Boltzmann constant and  $a$  a typical distance 182  
 183 between molecules). At  $T_g$ , which as a rule of thumb is 183  
 184 about  $2/3 T_m$ , the typical timescale has become of the or- 184  
 185 der of 100 s, i. e. 14 orders of magnitude larger! This phe- 185  
 186 nomenon is accompanied by a concomitant increase of 186  
 187 the shear viscosity  $\eta$ . This can be understood by a simple 187  
 188 Maxwell model in which  $\eta$  and  $\tau$  are related by  $\eta = G_\infty \tau_\alpha$ , 188  
 189 where  $G_\infty$  is the instantaneous (elastic) shear modu- 189  
 190 lus which does not vary considerably in the supercooled 190  
 191 regime. In fact, viscosities at the glass transition temper-

192 ature are of the order of  $10^{12}$  Pa.s. In order to grasp how  
 193 viscous this is, recall that the typical viscosity of water at  
 194 ambient temperature is of the order of  $10^{-2}$  Pa.s. How long  
 195 would one have to wait to drink a glass of water with a vis-  
 196 cosity  $10^{14}$  times larger?

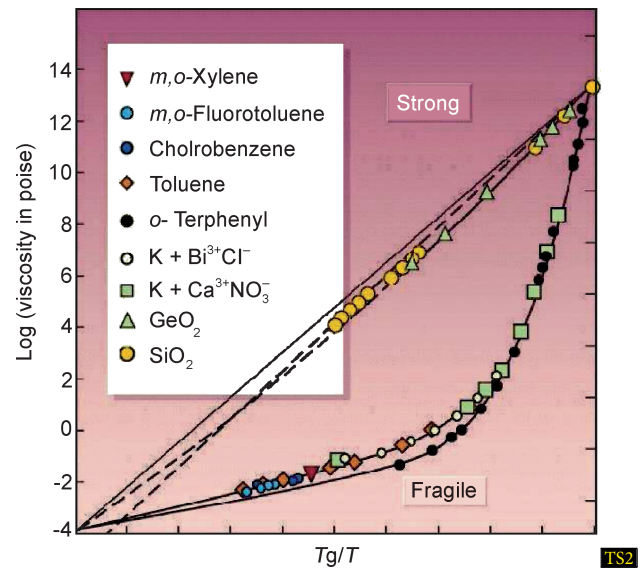
197 As a matter of fact, the temperature at which the liquid  
 198 does not flow anymore and becomes an amorphous solid,  
 199 called a ‘glass’, is protocol dependent. It depends on the  
 200 cooling rate and on the patience of the people carrying out  
 201 the experiment: solidity is a timescale dependent notion.  
 202 Pragmatically,  $T_g$  is defined as the temperature at which  
 203 the shear viscosity is equal to  $10^{13}$  Poise (also  $10^{12}$  Pa.s).

204 The increase of the relaxation timescale of supercooled  
 205 liquids is remarkable not only because of the large num-  
 206 ber of decades involved but also because of its tempera-  
 207 ture dependence. This is vividly demonstrated by plotting  
 208 the logarithm of the viscosity (or the relaxation time) as  
 209 a function of  $T_g/T$ , as in Fig. 1. This is called the ‘Angell’  
 210 plot [6] and is very helpful in classifying supercooled liq-  
 211 uids. A liquid is called strong or fragile depending on its  
 212 position in the Angell plot. Straight lines correspond to  
 213 ‘strong’ glass-formers and to an Arrhenius behaviour. In  
 214 this case, one can extract from the plot an effective activa-  
 215 tion energy, suggesting quite a simple mechanism for re-  
 216 laxation by ‘breaking’ locally a chemical bond. The typical  
 217 relaxation time is then dominated by the energy barrier to  
 218 activate this process and, hence, has an Arrhenius be-  
 219 haviour. Window glasses fall in this category<sup>1</sup>. If one tries  
 220 to define an effective activation energy for fragile glass-  
 221 formers using the slope of the curve in Fig. 1, then one  
 222 finds that this energy scale increases when the temperature  
 223 decreases, a ‘super-Arrhenius’ behaviour. This increase of  
 224 energy barriers immediately suggests that the glass forma-  
 225 tion is a collective phenomenon for fragile supercooled liq-  
 226 uids. Support for this interpretation is provided by the fact  
 227 that a good fit of the relaxation time or the viscosity is  
 228 given by the Vogel–Fulcher–Tamman law (VFT):

$$229 \quad \tau_\alpha = \tau_0 \exp \left[ \frac{DT_0}{(T - T_0)} \right], \quad (1)$$

230 which suggests a divergence of the relaxation time, and  
 231 therefore a phase transition of some kind, at a finite tem-  
 232 perature  $T_0$ . A smaller  $D$  in the VFT law corresponds to  
 233 a more fragile glass. Note that there are other comparably

<sup>1</sup>The terminology ‘strong’ and ‘fragile’ is not related to the mechanical properties of the glass but to the evolution of the short-range order close to  $T_g$ . Strong liquids, such as  $\text{SiO}_2$ , have a locally tetrahedral structure which persists both below and above the glass transition contrary to fragile liquids whose short-range amorphous structure disappears rapidly upon heating above  $T_g$ .



**Glasses and Aging: A Statistical Mechanics Perspective, Figure 1**  
 Arrhenius plot of the viscosity of several glass-forming liquids approaching the glass temperature  $T_g$  [67]. For ‘strong’ glasses, the viscosity increases in an Arrhenius manner as temperature is decreased,  $\log \eta \sim E/(K_B T)$ , where  $E$  is an activation energy and the plot is a straight line, as for silica. For ‘fragile’ liquids, the plot is bent and the effective activation energy increases when  $T$  is decreased towards  $T_g$ , as for ortho-terphenyl

234 good fits of these curves, such as the Bässler law [10],

$$235 \quad \tau_\alpha = \tau_0 \exp \left( K \left( \frac{T_*}{T} \right)^2 \right),$$

236 that only lead to a divergence at zero temperature. Actu-  
 237 ally, although the relaxation time increases by 14 orders of  
 238 magnitude, the increase of its logarithm, and therefore of  
 239 the effective activation energy is very modest, and experi-  
 240 mental data do not allow one to unambiguously determine  
 241 the true underlying functional law without any reasonable  
 242 doubt. For this and other reasons, physical interpretations  
 243 in terms of a finite temperature phase transition must al-  
 244 ways be taken with a grain of salt.

245 However, there are other experimental facts that shed  
 246 some light and reinforce this interpretation. Among them,  
 247 is an empirical connection found between kinetic and  
 248 thermodynamic behaviours. Consider the part of the en-  
 249 tropy of the liquids,  $S_{\text{exc}}$ , which is in excess compared to  
 250 the entropy of the corresponding crystal. Once this quan-  
 251 tity, normalized by its value at the melting temperature, is  
 252 plotted as a function of  $T$ , a remarkable connection with  
 253 the dynamics emerges. As for the relaxation time one can-  
 254 not follow this curve below  $T_g$  in thermal equilibrium.

**TS2** Please note that this figure will be printed in gray in the final version.

**Glasses and Aging: A Statistical Mechanics Perspective, Table 1**  
**Values of glass transition temperature, VFT singularity and Kauzmann temperatures for four supercooled liquids [145]**

Substance	o-ter-phenyl	2-methyltetrahydrofuran	n-propanol	3-bromopentane
$T_g$	246	91	97	108
$T_0$	202.4	69.6	70.2	82.9
$T_K$	204.2	69.3	72.2	82.5
$T_K/T_0$	1.009	0.996	1.028	0.995

255 However, extrapolating the curve below  $T_g$  apparently indicates that the excess entropy vanishes at some finite temperature, called  $T_K$ , which is very close to zero for strong glasses and, generically, very close to  $T_0$ , the temperature at which a VFT fit diverges. This coincidence is quite remarkable: for materials with glass transition temperatures that vary from 50 K to 1000 K the ratio  $T_K/T_0$  remains close to 1, up to a few percents. Examples reported in [145] are provided in Table 1. The chosen subscript for  $T_K$  stands for Kauzmann [108] which recognized  $T_K$  as a very important temperature in the glass phase diagram. Kauzmann further claimed that some change of behaviour (phase transition, crystal nucleation, etc.) must take place above  $T_K$ , because below  $T_K$  the entropy of the liquid, a disordered state of matter, becomes less than the entropy of the crystal, an ordered state of matter. This situation that seemed paradoxical at that time is not a serious problem. There is no general principle that would constraint the entropy of the liquid to be larger than that of the crystal. As a matter of fact, the crystallisation transition for hard spheres takes place precisely because the crystal becomes the state with the largest entropy at sufficiently high density [97].

278 On the other hand, the importance of  $T_K$  stands, partially because it is experimentally very close to  $T_0$ . Additionally, the quantity  $S_{exc}$  which vanishes at  $T_K$ , is thought to be a proxy for the so-called configurational entropy,  $S_c$ , which quantifies the number of metastable states. A popular physical picture due to Goldstein [91] is that close to  $T_g$  the system explores a part of the energy landscape (or configuration space) which is full of minima separated by barriers that increase when temperature decreases. The dynamic evolution in the energy landscape would then consist in a rather short equilibration inside the minima followed by ‘jumps’ between different minima. At  $T_g$  the barriers have become so large that the system remains trapped in one minimum, identified as one of the possible microscopic amorphous configurations of a glass. Following this interpretation, one can split the entropy into two parts. A first contribution is due to the fast relaxation inside

295 one minimum, a second counts the number of metastable states,  $S_c = \log N_{metastable}$ , which is called the ‘configurational’ entropy. Assuming that the contribution to the entropy due to the ‘vibrations’ around an amorphous glass configuration is not very different from the entropy of the crystal, one finds that  $S_{exc} \approx S_c$ . In that case,  $T_K$  would correspond to a temperature at which the configurational entropy vanishes. This in turn would lead to a discontinuity (a downward jump) of the specific heat and would truly correspond to a thermodynamic phase transition.

### Static and Dynamic Correlation Functions

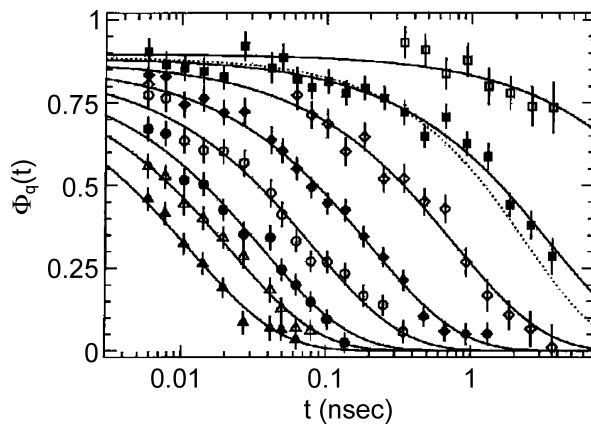
306 At this point the reader might have reached the conclusion that the glass transition may not be such a difficult problem: there are experimental indications of a diverging timescale and a concomitantly singularity in the thermodynamics. It simply remains to find static correlation functions displaying a diverging correlation length related to the emergence of ‘amorphous order’, which would indeed classify the glass transition as a standard second order phase transition. Remarkably, this remains an open and debated question despite several decades of research. Simple static correlation function are quite featureless in the supercooled regime, notwithstanding the dramatic changes in the dynamics. A simple static quantity is the structure factor defined by

$$S(q) = \left\langle \frac{1}{N} \delta\rho_{\mathbf{q}} \delta\rho_{-\mathbf{q}} \right\rangle ,$$

where the Fourier component of the density reads

$$\delta\rho_{\mathbf{q}} = \sum_{i=1}^N e^{i\mathbf{q}\cdot\mathbf{r}_i} - \frac{N}{V} \delta_{\mathbf{q},0} ,$$

323 with  $N$  is the number of particles,  $V$  the volume, and  $\mathbf{r}_i$  is the position of particle  $i$ . The structure factor measures the spatial correlations of particle positions, but it does not show any diverging peak in contrast to what happens, for example, at the liquid-gas tri-critical point where there is a divergence at small  $\mathbf{q}$ . More complicated static correlation functions have been studied [66], especially in numerical work, but until now there are no strong indications of a diverging, or at least substantially growing, static lengthscale [133]. A snapshot of a supercooled liquid configuration in fact just looks like a glass configuration, despite their widely different dynamic properties. What happens then at the glass transition? Is it a transition or simply a dynamic crossover? A more refined understanding can be gained studying dynamic correlations or response functions.



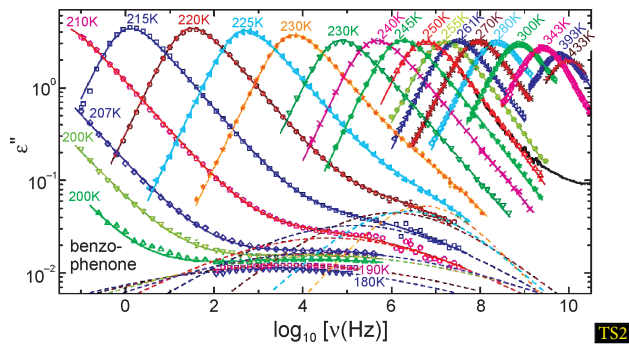
**Glasses and Aging: A Statistical Mechanics Perspective, Figure 2** Temperature evolution of the intermediate scattering function normalized by its value at time equal to zero for supercooled glycerol [170]. Temperatures decrease from 413 K to 270 K from right to left. The solid lines are fit with a stretched exponential with exponent  $\beta = 0.7$ . The dotted line represents another fit with  $\beta = 0.82$

A dynamic observable studied in light and neutron scattering experiments is the intermediate scattering function,

$$F(\mathbf{q}, t) = \left\langle \frac{1}{N} \delta\rho_{\mathbf{q}}(t) \delta\rho_{-\mathbf{q}}(0) \right\rangle. \quad (2)$$

Different  $F(\mathbf{q}, t)$  measured by neutron scattering in supercooled glycerol [170] are shown for different temperatures in Fig. 2. These curves show a first, rather fast, relaxation to a plateau followed by a second, much slower, relaxation. The plateau is due to the fraction of density fluctuations that are frozen on intermediate timescales, but eventually relax during the second relaxation. The latter is called ‘alpha-relaxation’, and corresponds to the structural relaxation of the liquid. This plateau is akin to the Edwards–Anderson order parameter,  $q_{EA}$ , defined for spin glasses which measures the fraction of frozen spin fluctuations [33]. Note that  $q_{EA}$  continuously increases from zero below the spin glass transition. Instead, for structural glasses, a finite plateau appears above any transition.

The intermediate scattering function can be probed only on a relatively small regime of temperatures. In order to track the dynamic slowing down from microscopic to macroscopic timescales, other correlators have been studied. A popular one is obtained from the dielectric susceptibility, which is related by the fluctuation-dissipation theorem to the time correlation of polarization fluctuations. It is generally admitted that different dynamic probes reveal similar temperature dependences for the relaxation time. The temperature evolution of the imagi-



**Glasses and Aging: A Statistical Mechanics Perspective, Figure 3** Temperature evolution of the dielectric susceptibility of the glass-former benzophenone measured over more than 10 decades of relaxation times [142]. Dynamics slows down dramatically as temperature is decreased and relaxation spectra become very broad at low temperature

nary part of the dielectric susceptibility,  $\epsilon''(\omega)$ , is shown in Fig. 3 which covers a very wide temperature window [142]. At high temperature, a good representation of the data is given by a Debye law,  $\epsilon(\omega) = \epsilon(\infty) + \Delta\epsilon/(1 + i\omega\tau_\alpha)$ , which corresponds to an exponential relaxation in the time domain. When temperature is decreased, however, the relaxation spectra become very broad and strongly non-Debye. One particularly well-known feature of the spectra is that they are well fitted, in the time domain, for times corresponding to the alpha-relaxation with a stretched exponential,  $\exp(-(t/\tau_\alpha)^\beta)$ . In the Fourier domain, forms such as the Havriliak–Negami law are used,  $\epsilon(\omega) = \epsilon(\infty) + \Delta\epsilon/(1 + (i\omega\tau_\alpha)^\alpha)^\gamma$ , which generalizes the Debye law. The exponents  $\beta$ ,  $\alpha$  and  $\gamma$  depend in general on temperature and on the particular dynamic probe chosen, but they capture the fact that relaxation is increasingly non-exponential when  $T$  decreases towards  $T_g$ . A connection was empirically established between fragility and degree of non-exponentiality, more fragile liquids being characterized by broader relaxation spectra [67].

To sum up, there are many remarkable phenomena that take place when a supercooled liquid approaches the glass transition. Striking ones have been presented, but many others have been left out for lack of space [6,33,66, 67]. We have discussed physical behaviours, relationships or empirical correlations observed in a broad class of materials. This is quite remarkable and suggests that there is some physics (and not only chemistry) to the problem of the glass transition, which we see as a collective (critical?) phenomenon which is relatively independent of microscopic details. This justifies our statistical mechanics perspective on this problem.

### 399 Taxonomy of ‘Glasses’ in Science

400 We now introduce some other systems whose phe-  
 401 nomenological behaviour is close or, at least, related, to  
 402 the one of glass-forming liquids, showing that glassiness  
 403 is truly ubiquitous. It does not only appear in many differ-  
 404 ent physical situations but also in more abstract contexts,  
 405 such as computer science.

### 406 The Jamming Transition of Colloids and Grains

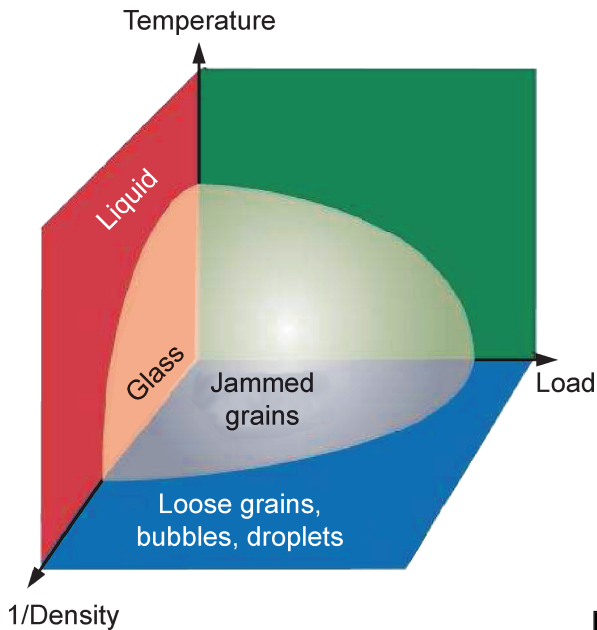
407 Colloidal suspensions consist of big particles suspended  
 408 in a solvent [121]. The typical radii of the particles are in  
 409 the range  $R = 1\text{--}500$  nm. The solvent, which is at equilib-  
 410 rium at temperature  $T$ , renders the short-time dynamics  
 411 of the particles Brownian. The microscopic timescale for  
 412 this diffusion is given by  $\tau = R^2/D$  where  $D$  is the short-  
 413 time self-diffusion coefficient. Typical values are of the or-  
 414 der of  $\tau \sim 1$  ms, and thus are much larger than the ones for  
 415 molecular liquids (in the picosecond regime). The interac-  
 416 tion potential between particles depends on the systems,  
 417 and this large tunability makes colloids very attractive  
 418 objects for technical applications. A particularly relevant  
 419 case, on which we will focus in the following, is a purely  
 420 hard sphere potential, which is zero when particles do not  
 421 overlap and infinite otherwise. In this case the tempera-  
 422 ture becomes irrelevant, apart from a trivial rescaling of  
 423 the microscopic timescale. Colloidal hard spheres systems  
 424 have been intensively studied [121] in experiments, sim-  
 425 ulations and theory varying their density  $\rho$ , or their vol-  
 426 ume fraction  $\phi = 4/3\pi R^3\rho$ . Hard spheres display a fluid  
 427 phase from 0 to intermediate volume fractions, a freezing-  
 428 crystallisation transition at  $\phi \simeq 0.494$ , and a melting tran-  
 429 sition at  $\phi \simeq 0.545$ . Above this latter value the system  
 430 can be compressed until the close packing point  $\phi \simeq 0.74$ ,  
 431 which corresponds to the FCC crystal. Interestingly for  
 432 our purposes, a small amount of polydispersity (particles  
 433 with slightly different sizes) suppresses crystallization. In  
 434 this case, the system can be more easily ‘supercompressed’  
 435 above the freezing transition without nucleating the crys-  
 436 tal, at least on experimental timescales. In this regime the  
 437 relaxation timescale increases very fast [144]. At a pack-  
 438 ing fraction  $\phi_g \simeq 0.58$  it becomes so large compared to  
 439 typical experimental timescales that the system does not  
 440 relax anymore: it is jammed. This ‘jamming transition’ is  
 441 obviously reminiscent of the glass transition of molecular  
 442 systems. In particular, the location  $\phi_g$  of the colloidal glass  
 443 transition is as ill-defined as the glass temperature  $T_g$ .

444 Actually, the phenomena that take place increas-  
 445 ing the volume fraction are analogous to the ones seen in  
 446 molecular supercooled liquid: the relaxation timescales in-  
 447 creases very fast and can be fitted [52] by a VFT law in

448 density as in Eq. (1), dynamical correlation functions dis-  
 449 play a broad spectrum of timescales and develop a plateau,  
 450 no static growing correlation length has been found, etc.  
 451 Also the phenomenon of dynamic heterogeneity that will  
 452 be addressed in Sect. “Dynamic Heterogeneity” is present  
 453 in both cases [109,165]. However, it is important to under-  
 454 line a major difference: because the microscopic timescale  
 455 for colloids is so large, experiments can only track the  
 456 first 5 decades of slowing down. A major consequence is  
 457 that the comparison between the glass and colloidal tran-  
 458 sitions must be performed by focusing in both cases on the  
 459 first 5 decades of the slowing down, which corresponds to  
 460 relatively high temperatures in molecular liquids. Under-  
 461 standing how much and to what extent the glassiness of  
 462 colloidal suspensions is related to the one of molecular liq-  
 463 uids remains an active domain of research.

464 Another class of systems that have recently been stud-  
 465 ied from the point of view of their glassiness is driven gran-  
 466 ular media. Grains are macroscopic objects and, as a con-  
 467 sequence, do not have any thermal motion. A granular ma-  
 468 terial is therefore frozen in a given configuration if no en-  
 469 ergy is injected into the system [104]. However, it can be  
 470 forced in a steady state by an external drive, such as shear-  
 471 ing or tapping. The dynamics in this steady state shows  
 472 remarkable similarities (and differences) with simple flu-  
 473 ids. The physics of granular materials is a very wide sub-  
 474 ject [104]. In the following we only address briefly what  
 475 happens to a polydisperse granular fluid at very high pack-  
 476 ing fractions, close to its random close packed state. As for  
 477 colloids, the timescales for relaxation or diffusion increase  
 478 very fast when density is increased, without any notice-  
 479 able change in structural properties. Again, it is now es-  
 480 tablished [62,110,127] that many phenomenological prop-  
 481 erties of the glass and jamming transitions also occur in  
 482 granular assemblies. As for colloids, going beyond the  
 483 mere analogy and understanding how much these differ-  
 484 ent physical systems are related is a very active domain of  
 485 research.

486 This very question has been asked in a visual manner  
 487 by Liu and Nagel [124] who rephrased it in a single picture,  
 488 reproduced in Fig. 4. By building a common phase dia-  
 489 gram for glasses, colloids and grains, they ask whether the  
 490 glass and jamming transitions of molecular liquids, col-  
 491 loids and granular media are different facets of the same  
 492 phase. In this unifying ‘phase diagram’, the ‘phase’ close  
 493 to the origin is glassy and can be reached either by low-  
 494 ering the temperature as in molecular liquids, or increas-  
 495 ing the packing fraction or decreasing the external drive in  
 496 colloids and granular media. It remains to provide precise  
 497 answers to this elegantly formulated, but rather broad, set  
 498 of questions.



Glasses and Aging: A Statistical Mechanics Perspective, Figure 4 The 'great unification' phase diagram of jamming and glass transitions [124]. Glassy phases occur at low temperature, low external drive, or high density in different systems

#### Other 'Glasses' in Physics and Beyond

There are many other physical contexts in which glassiness plays an important role [173]. One of the most famous examples is the field of spin glasses. Real spin glasses are magnetic impurities interacting by quenched random couplings. At low temperatures, their dynamics become extremely slow and they freeze in amorphous spin configuration dubbed a 'spin glass' by P. W. Anderson. There are many other physical systems, often characterized by quenched disorder, that show glassy behaviour, like Coulomb glasses, Bose glasses, etc. In many cases, however, one does expect quite a different physics from structural glasses: the similarity between these systems is therefore only qualitative.

Finally, and quite remarkably, glassiness emerges even in other branches of science [55]. In particular, it has been discovered recently that concepts and techniques developed for glassy systems turn out to apply and be very useful tools in the field of computer science. Problems like combinatorial optimization display phenomena completely analogous to phase transitions, actually, to glassy phase transitions. A posteriori, this is quite natural, because a typical optimization problem consists in finding a solution in a presence of a large number of constraints. This can be defined, for instance, as a set of  $N$  Boolean

variables that satisfies  $M$  constraints. For  $N$  and  $M$  very large at fixed  $\alpha = M/N$ , this problem very much resembles finding a ground state in a statistical mechanics problem with quenched disorder. Indeed one can define an energy function (a Hamiltonian) as the number of unsatisfied constraints, that has to be minimized, as in a  $T = 0$  statmech problem. The connection with glassy systems originates from the fact that in both cases the energy landscape is extremely complicated, full of minima and saddles. The fraction of constraints per degree of freedom,  $\alpha$ , plays a role similar to the density in a hard sphere system. A detailed presentation of the relationship between optimization problems and glassy systems is clearly out of the scope of the present review. We simply illustrate it pointing out that a central problem in optimization, random  $k$ -satisfiability, has been shown to undergo a glass transition when  $\alpha$  increases that is analogous to the one of structural glasses [117].

TS2

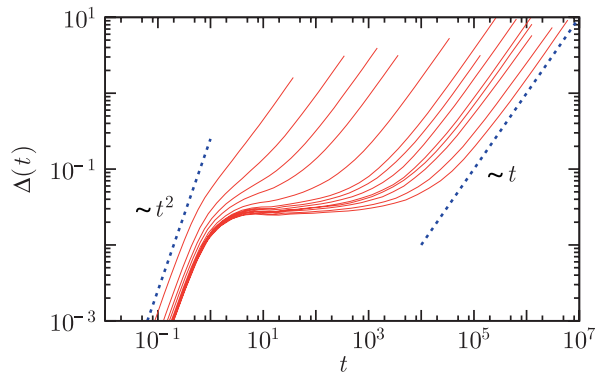
#### Numerical Simulations

Studying the glass transition of molecular liquids at a microscopic level is in principle straightforward since one must answer a very simple question: how do particles move in a liquid close to  $T_g$ ? It is of course a daunting task to attempt answering this question experimentally because one should then resolve the dynamics of single molecules to be able to follow the trajectories of objects that are a few Angstroms large on timescales of tens or hundreds of seconds, which sounds like eternity when compared to typical molecular dynamics usually lying in the picosecond regime. In recent years, such direct experimental investigations have been started using time and space resolved techniques such as atomic force microscopy [161] or single molecule spectroscopy [3], but this remains a very difficult task.

In numerical simulations, by contrast, the trajectory of each particle in the system can, by construction, be followed at all times. This allows one to quantify easily single particle dynamics, as proved in Fig. 5 where the averaged mean-squared displacement  $\Delta(t)$  measured in a simple Lennard-Jones glass-former is shown. It is defined by

$$\Delta(t) = \left\langle \frac{1}{N} \sum_{i=1}^N |\mathbf{r}_i(t) - \mathbf{r}_i(0)|^2 \right\rangle,$$

where  $\mathbf{r}_i(t)$  represents the position of particle  $i$  at time  $t$  in a system composed of  $N$  particles; the brackets indicate an ensemble average. The particle displacements considerably slow down when  $T$  is decreased and the self-diffusion constant decreases by orders of magnitude, mirroring the behaviour of the viscosity shown in Fig. 1 for



**Glasses and Aging: A Statistical Mechanics Perspective, Figure 5** Mean-squared displacements of individual particles in a simple model of a glass-forming liquid composed of Lennard-Jones particles observed on a wide time window. When temperature decreases (from left to right), the particle displacements become increasingly slow with several distinct time regimes corresponding, in this order, to ballistic, localized, and diffusive regimes

571 real systems. Moreover, a rich dynamics is observed, with  
 572 a plateau regime at intermediate timescales, correspond-  
 573 ing to an extended time window during which particles  
 574 vibrate around their initial positions, exactly as in a crys-  
 575 talline solid. The difference with a crystal is of course that  
 576 this localization is only transient, and all particles eventu-  
 577 ally escape and diffuse at long times with a diffusion con-  
 578 stant  $D_s$ , so that  $\Delta(t) \sim 6D_s t$  when  $t \rightarrow \infty$ .

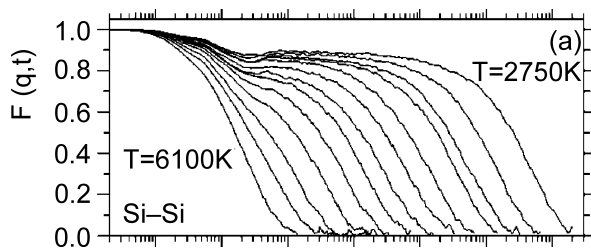
579 In recent years, computer experiments have played an  
 580 increasingly important role in glass transition studies. It  
 581 could almost be said that particle trajectories in numeri-  
 582 cal work have been studied under so many different an-  
 583 gles that probably very little remains to be learnt from  
 584 such studies in the regime that is presently accessible using  
 585 present day computers. Unfortunately, this does not imply  
 586 complete knowledge of the physics of supercooled liquids.  
 587 As shown in Fig. 5, it is presently possible to follow the  
 588 dynamics of a simple glass-forming liquid over more than  
 589 eight decades of time, and over a temperature window in  
 590 which average relaxation timescales increase by more than  
 591 five decades. This might sound impressive, but a quick  
 592 look at Fig. 1 shows, however, that at the lowest temper-  
 593 atures studied in the computer, the relaxation timescales  
 594 are still orders of magnitude faster than in experiments  
 595 performed close to the glass transition temperature. They  
 596 can be directly compared to experiments performed in this  
 597 high temperature regime, but this also implies that sim-  
 598 ulations focus on a relaxation regime that is about eight  
 599 to ten decades of times faster than in experiments per-  
 600 formed close to  $T_g$ . Whether numerical works are useful to  
 601 understand the glass transition itself at all is therefore an

open, widely debated, question. We believe that it is now  
 possible to numerically access temperatures which are low  
 enough that many features associated to the glass transi-  
 tion physics can be observed: strong decoupling phenom-  
 ena, clear deviations from fits to the mode-coupling the-  
 ory (which are experimentally known to hold only at high  
 temperatures), and crossovers towards truly activated dy-  
 namics.

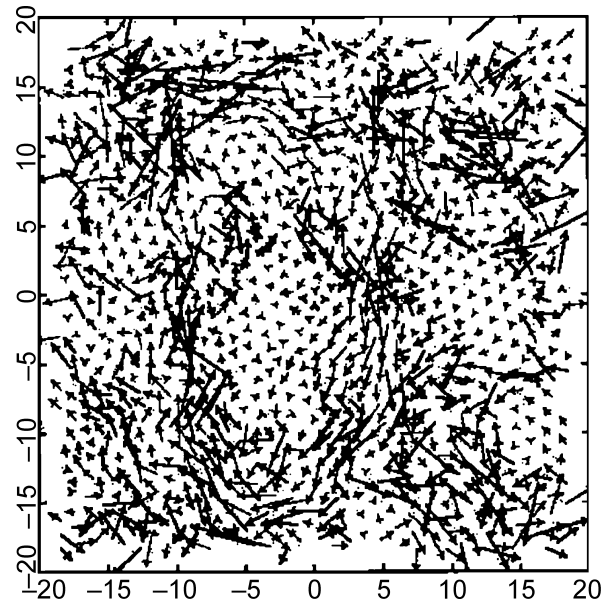
Classical computer simulations of supercooled liquids  
 usually proceed by solving a cleverly discretized version  
 of Newton's equations for a given potential interaction  
 between particles [4]. If quantitative agreement with ex-  
 perimental data on an existing specific material is sought,  
 the interaction must be carefully chosen in order to re-  
 produce reality, for instance by combining classical to ab  
 initio simulations. From a more fundamental perspective  
 one rather seeks the simplest model that is still able to  
 reproduce qualitatively the phenomenology of real glass-  
 formers, while being considerably simpler to study. The  
 implicit, but quite strong, hypothesis is that molecular de-  
 tails are not needed to explain the behaviour of super-  
 cooled liquids, so that the glass transition is indeed a topic  
 for statistical mechanics, not for chemistry. A considerable  
 amount of work has therefore been dedicated to studying  
 models such as hard spheres, soft spheres, or Lennard-  
 Jones particles. More realistic materials are also studied  
 focusing for instance on the physics of network forming  
 materials, multi-component ones, anisotropic particles, or  
 molecules with internal degrees of freedom. Connections  
 to experimental work can be made by computing quanti-  
 ties that are experimentally accessible such as the interme-  
 diate scattering function, static structure factors,  $S(\mathbf{q})$ , or  
 thermodynamic quantities such specific heat or configura-  
 tional entropy, which are directly obtained from particle  
 trajectories and can be measured in experiments as well.  
 As an example we show in Fig. 6 the intermediate scatter-  
 ing function  $F(\mathbf{q}, t)$  obtained from a molecular dynamics  
 simulation of a classical model for  $\text{SiO}_2$  as a function of  
 time for different temperatures [98].

An important role is played by simulations also be-  
 cause a large variety of dynamic and static quantities can  
 be simultaneously measured in a single model system. As  
 we shall discuss below, there exist scores of different theo-  
 retical approaches to describe the physics of glass-formers,  
 and they sometimes have their own set of predictions that  
 can be readily tested by numerical work. Indeed, quite  
 a large amount of numerical papers have been dedicated to  
 testing in detail the predictions formulated by the mode-  
 coupling theory of the glass transition, as reviewed re-  
 cently in [94]. Here, computer simulations are particularly  
 well-suited as the theory specifically addresses the rela-





**Glasses and Aging: A Statistical Mechanics Perspective, Figure 6** Intermediate scattering function at wavevector  $1.7 \text{ \AA}^{-1}$  for the Si particles at  $T = 2750 \text{ K}$  obtained from molecular dynamics simulations of a model for silica [98]



**Glasses and Aging: A Statistical Mechanics Perspective, Figure 7** Spatial map of single particle displacements in the simulation of a binary mixture of soft spheres in two dimensions [99]. Arrows show the displacement of each particle in a trajectory of length about 10 times the structural relaxation time. The map reveals the existence of particles with different mobilities during relaxation, but also the existence of spatial correlations between these dynamic fluctuations

653 tively high temperature window that is studied in com-  
654 puter simulations.

655 While Newtonian dynamics is mainly used in numerical  
656 work on supercooled liquids, a most appropriate choice  
657 for these materials, it can be interesting to consider alter-  
658 native dynamics that are not deterministic, or which do  
659 not conserve the energy. In colloidal glasses and phys-  
660 ical gels, for instance, particles undergo Brownian mo-  
661 tion arising from collisions with molecules in the solvent,  
662 and a stochastic dynamics is more appropriate. Theoret-  
663 ical considerations might also suggest the study of dif-  
664 ferent sorts of dynamics for a given interaction between  
665 particles, for instance, to assess the role of conservation  
666 laws and structural information. Of course, if a given dy-  
667 namics satisfies detailed balance with respect to the Boltz-  
668 mann distribution, all structural quantities remain un-  
669 changed, but the resulting dynamical behaviour might be  
670 very different. Several papers [27,88,153] have studied in  
671 detail the influence of the chosen microscopic dynamics  
672 on the dynamical behaviour in glass-formers using either  
673 stochastic dynamics (where a friction term and a random  
674 noise are added to Newton's equations, the amplitude of  
675 both terms being related by a fluctuation-dissipation the-  
676 orem), Brownian dynamics (in which there are no mo-  
677 menta, and positions evolve with Langevin dynamics), or  
678 Monte-Carlo dynamics (where the potential energy be-  
679 tween two configurations is used to accept or reject a trial  
680 move). Quite surprisingly, the equivalence between these  
681 three types of stochastic dynamics and the originally stud-  
682 ied Newtonian dynamics was established at the level of  
683 the averaged dynamical behaviour [27,88,153], except at  
684 very short times where obvious differences are indeed ex-  
685 pected. This strongly suggests that an explanation for the  
686 appearance of slow dynamics in these materials originates  
687 from their amorphous structure. However, important dif-  
688 ferences were found when dynamic fluctuations were con-

688 sidered [21,22,27], even in the long-time regime compris-  
689 ing the structural relaxation.

690 Another crucial advantage of molecular simulations is  
691 illustrated in Fig. 7. This figure shows a spatial map of sin-  
692 gle particle displacements recorded during the simulation  
693 of a binary soft sphere system in two dimensions [99]. This  
694 type of measurement, out of reach of most experimental  
695 techniques that study the liquid state, reveals that dynam-  
696 ics might be very different from one particle to another.  
697 More importantly, Fig. 7 also unambiguously reveals the  
698 existence of spatial correlations between these dynamic  
699 fluctuations. The presence of non-trivial spatio-temporal  
700 fluctuations in supercooled liquids is now called 'dynamic  
701 heterogeneity' [72]. This is the phenomenon we discuss in  
702 more detail in the next section.

### 703 Dynamic Heterogeneity

#### 704 Existence of Spatio-temporal Dynamic Fluctuations

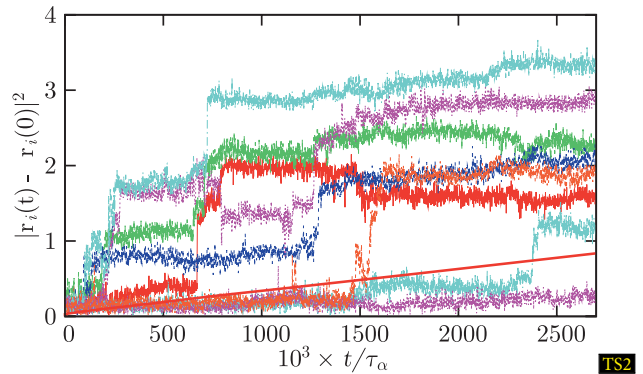
705 A new facet of the relaxational behaviour of supercooled  
706 liquids has emerged in the last decade thanks to a consid-  
707 erable experimental and theoretical effort. It is called 'dy-  
708 namic heterogeneity' (DH), and plays now a central role

709 in modern descriptions of glassy liquids [72]. As anti-  
 710 cipated in the previous section, the phenomenon of dynamic  
 711 heterogeneity is related to the spatio-temporal fluctuations  
 712 of the dynamics. Initial motivations stemmed from the  
 713 search for an explanation of the non-exponentiality of re-  
 714 laxation processes in supercooled liquids, related to the ex-  
 715 istence of a broad relaxation spectrum. Two natural, but  
 716 fundamentally different, explanations can be put forward.  
 717 (1) The relaxation is locally exponential, but the typical re-  
 718 laxation timescale varies spatially. Hence, global correla-  
 719 tion or response functions become non-exponential upon  
 720 spatial averaging over this spatial distribution of relaxation  
 721 times. (2) The relaxation is complicated and inherently  
 722 non-exponential, even locally. Experimental and theoret-  
 723 ical works [72] suggest that both mechanisms are likely to  
 724 play, but definitely conclude that relaxation is spatially het-  
 725 erogeneous, with regions that are faster and slower than  
 726 the average. Since supercooled liquids are ergodic materi-  
 727 als, a slow region will eventually become fast, and vice  
 728 versa. A physical characterization of DH entails the deter-  
 729 mination of the typical lifetime of the heterogeneities, as  
 730 well as their typical lengthscale.

731 A clear and more direct confirmation of the heteroge-  
 732 nous character of the dynamics also stems from simu-  
 733 lation studies. For example, whereas the simulated aver-  
 734 age mean-squared displacements are smooth functions of  
 735 time, time signals for individual particles clearly exhibit  
 736 specific features that are not observed unless dynamics is  
 737 resolved both in space and time. These features are dis-  
 738 played in Fig. 8. What do we see? We mainly observe that  
 739 particle trajectories are not smooth but rather composed  
 740 of a succession of long periods of time where particles  
 741 simply vibrate around well-defined locations, separated by  
 742 rapid ‘jumps’. Vibrations were previously inferred from  
 743 the plateau observed at intermediate times in the mean-  
 744 squared displacements of Fig. 5, but the existence of jumps  
 745 that are clearly statistically widely distributed in time can-  
 746 not be guessed from averaged quantities only. The fluctu-  
 747 ations in Fig. 8 suggest, and direct measurements confirm,  
 748 the importance played by fluctuations around the averaged  
 749 dynamical behaviour.

750 A simple type of such fluctuations has been studied in  
 751 much detail. When looking at Fig. 8, it is indeed natural to  
 752 ask, for any given time, what is the distribution of parti-  
 753 cle displacements. This is quantified by the self-part of the  
 754 van-Hove function defined as

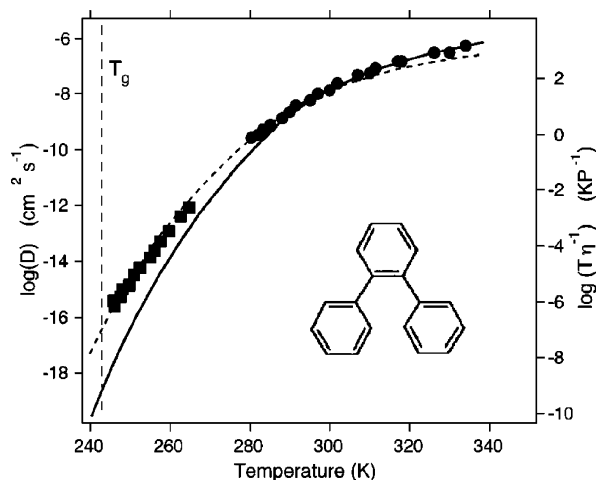
$$755 \quad G_s(\mathbf{r}, t) = \left\langle \frac{1}{N} \sum_{i=1}^N \delta(\mathbf{r} - [\mathbf{r}_i(t) - \mathbf{r}_i(0)]) \right\rangle.$$



**Glasses and Aging: A Statistical Mechanics Perspective, Figure 8**  
 Time resolved squared displacements of individual particles in a simple model of a glass-forming liquid composed of Lennard-Jones particles. The average is shown as a smooth full line. Trajectories are composed of long periods of time during which particles vibrate around well-defined positions, separated by rapid jumps that are widely distributed in time underlying the importance of dynamic fluctuations

756 For an isotropic Gaussian diffusive process, one gets  
 757  $G_s(\mathbf{r}, t) = \exp(-|\mathbf{r}|^2/(4D_s t))/(4\pi D_s t)^{3/2}$ . Simulations re-  
 758 veal instead strong deviations from Gaussian behaviour  
 759 on the timescales relevant for structural relaxation [116].  
 760 In particular they reveal ‘fat’ tails in the distributions that  
 761 are much wider than expected from the Gaussian approxi-  
 762 mation. These tails are in fact well described by an ex-  
 763 ponential, rather than Gaussian, decay in a wide time  
 764 window comprising the structural relaxation, such that  
 765  $G_s(\mathbf{r}, t) \sim \exp(-|\mathbf{r}|/\lambda(t))$  [51]. Thus, they reflect the exis-  
 766 tence of a population of particles that moves distinctively  
 767 further than the rest and appears therefore to be much  
 768 more mobile. This observation implies that relaxation in  
 769 a viscous liquid differs qualitatively from that of a normal  
 770 liquid where diffusion is close to Gaussian, and that a non-  
 771 trivial statistics of single particle displacements exists.

772 A long series of questions immediately follows this  
 773 seemingly simple observation. Answering them has been  
 774 the main occupation of many workers in this field over  
 775 the last decade. What are the particles in the tails effec-  
 776 tively doing? Why are they faster than the rest? Are they  
 777 located randomly in space or do they cluster? What is  
 778 the geometry, time and temperature evolution of the clus-  
 779 ters? Are these spatial fluctuations correlated to geomet-  
 780 ric or thermodynamic properties of the liquids? Do sim-  
 781 ilar correlations occur in all glassy materials? Can one  
 782 predict these fluctuations theoretically? Can one under-  
 783 stand glassy phenomenology using fluctuation-based ar-  
 784 guments? Can these fluctuations be detected experimen-  
 785 tally?



**Glasses and Aging: A Statistical Mechanics Perspective, Figure 9** Decoupling between viscosity (full line) and self-diffusion coefficient (symbols) in supercooled ortho-terphenyl [126] The dashed line shows a fit with a 'fractional' Stokes-Einstein relation,  $D_s \sim (T/\eta)^\zeta$  with  $\zeta \sim 0.82$

Another influential phenomenon that was related early on to the existence of DH is the decoupling of self-diffusion ( $D_s$ ) and viscosity ( $\eta$ ). In the high temperature liquid self-diffusion and viscosity are related by the Stokes-Einstein relation [95],  $D_s\eta/T = \text{const}$ . For a large particle moving in a fluid the constant is equal to  $1/(6\pi R)$  where  $R$  is the particle radius. Physically, the Stokes-Einstein relation means that two different measures of the relaxation time  $R^2/D_s$  and  $\eta R^3/T$  lead to the same timescale up to a constant factor. In supercooled liquids this phenomenological law breaks down, as shown in Fig. 9 for ortho-terphenyl [126]. It is commonly found that  $D_s^{-1}$  does not increase as fast as  $\eta$  so that, at  $T_g$ , the product  $D_s\eta$  has increased by 2–3 orders of magnitude as compared to its Stokes-Einstein value. This phenomenon, although less spectacular than the overall change of viscosity, is a significant indication that different ways to measure relaxation times lead to different answers and, thus, is a strong hint of the existence of a distribution of relaxation timescales.

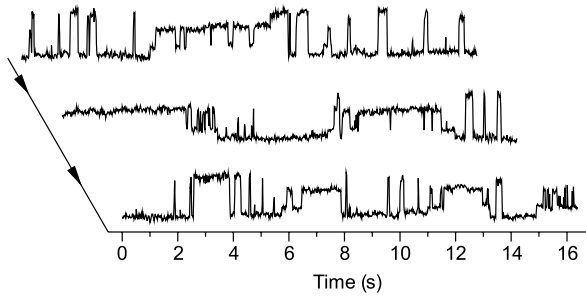
Indeed, a natural explanation of this effect is that different observables probe differently way the underlying distribution of relaxation times [72]. For example, the self-diffusion coefficient of tracer particles is dominated by the more mobile particles whereas the viscosity or other measures of structural relaxation probe the timescale needed for every particle to move. An unrealistic but instructive example is a model where there is a small, non-percolative subset of particles that are blocked forever, coexisting with

a majority of mobile particles. In this case, the structure never relaxes but the self-diffusion coefficient is non-zero because of the mobile particles. Of course, in reality all particles move, eventually, but this shows how different observables are likely to probe different moments of the distribution of timescales, as explicitly shown within several theoretical frameworks [106,154].

The phenomena described above, although certainly an indication of spatio-temporal fluctuations, do not allow one to study how these fluctuations are correlated in space. This is, however, a fundamental issue both from the experimental and theoretical points of view. How large are the regions that are faster or slower than the average? How does their size depend on temperature? Are these regions compact or fractal? These important questions were first addressed in pioneering works using four-dimensional NMR [160], or by directly probing fluctuations at the nanoscopic scale using microscopy techniques. In particular, Vidal Russel and Israeloff using Atomic Force Microscopy techniques [161] measured the polarization fluctuations in a volume of size of few tens of nanometers in a supercooled polymeric liquid (PVAc) close to  $T_g$ . In this spatially resolved measurement, the hope is to probe a small enough number of dynamically correlated regions, and detect their dynamics. Indeed, the signal shown in Fig. 10 shows a dynamics which is very intermittent in time, the dynamics switching between moments with intense activity, and moments with no dynamics at all, suggesting that extended regions of space indeed transiently behave as fast and slow regions. A much smoother signal would have been measured if these such dynamically correlated 'domains' were not present. Spatially resolved and NMR experiments are quite difficult. They give undisputed information about the typical lifetime of the DH, but their determination of a dynamic correlation lengthscale is rather indirect and/or performed on a small number of liquids in a small temperature window. Nevertheless, the outcome is that a non-trivial dynamic correlation length emerges at the glass transition, where it reaches a value of the order of 5–10 molecule diameters [72].

### Multi-point Correlation Functions

More recently, substantial progress in characterizing spatio-temporal dynamical fluctuations was obtained from theoretical [21,22,79,159] and numerical results [14, 28,76,99,172]. In particular, it is now understood that dynamical fluctuations can be measured and characterized through the use of four-point correlation functions. These multi-point functions can be seen as a generalization of



**Glasses and Aging: A Statistical Mechanics Perspective, Figure 10**  
Time series of polarization in the AFM experiment performed by Vidal Russell and Israeloff [161] on PVAc at  $T=300$  K. The signal intermittently switches between periods with fast or slow dynamics, suggesting that extended regions of space indeed transiently behave as fast and slow regions

the spin glass susceptibility measuring the extent of amorphous long-range order in spin glasses. In this subsection, we introduce these correlation functions and summarize the main results obtained using them.

Standard experimental probes of the averaged dynamics of liquids give access to the time-dependent auto-correlation function of the spontaneous fluctuations of some observable  $O(t)$ ,  $F(t) = \langle \delta O(0)\delta O(t) \rangle$ , where  $\delta O(t) = O(t) - \langle O \rangle$  represents the instantaneous value of the deviation of  $O(t)$  from its ensemble average  $\langle O \rangle$  at time  $t$ . One can think of  $F(t)$  as being the average of a two-point quantity,  $C(0, t) = \delta O(0)\delta O(t)$ , characterizing the dynamics. A standard example corresponds to  $O$  being equal to the Fourier transform of the density field. In this case  $F(t)$  is the dynamical structure factor as in Eq. (2). More generally, the correlation functions  $F(t)$  measure the global relaxation in the system. Intuitively, in a system with important dynamic correlations, the fluctuations of  $C(0, t)$  be stronger. Quantitative information on the amplitude of those fluctuations is provided by the variance

$$\chi_4(t) = N \langle \delta C(0, t)^2 \rangle, \quad (3)$$

where  $\delta C(0, t) = C(0, t) - F(t)$ , and  $N$  is the total number of particles in the system. The associated spatial correlations show up more clearly when considering a 'local' probe of the dynamics, like for instance an orientational correlation function measured by dielectric or light scattering experiments, which can be expressed as

$$C(0, t) = \frac{1}{V} \int d^3r c(\mathbf{r}; 0, t), \quad (4)$$

where  $V$  is the volume of the sample and  $c(\mathbf{r}; 0, t)$  characterizes the dynamics between times 0 and  $t$  around point  $\mathbf{r}$ . For example, in the above mentioned case of

orientational correlations,  $c(\mathbf{r}; 0, t) \propto \frac{1}{N} \sum_{i,j=1}^N \delta(\mathbf{r} - \mathbf{r}_i) Y(\Omega_i(0)) Y(\Omega_j(t))$ , where  $\Omega_i$  denotes the angles describing the orientation of molecule  $i$ ,  $\mathbf{r}_i(0)$  is the position of that molecule at time 0, and  $Y(\Omega)$  is some appropriate rotation matrix element. Here, the 'locality' of the probe comes from the fact that it is dominated by the self-term involving the same molecule at times 0 and  $t$ , or by the contribution coming from neighboring molecules. The dynamic susceptibility  $\chi_4(t)$  can thus be rewritten as

$$\chi_4(t) = \rho \int d^3r G_4(\mathbf{r}; 0, t), \quad (5)$$

where

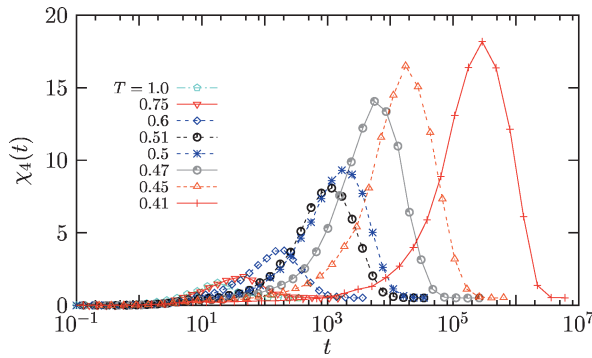
$$G_4(\mathbf{r}; 0, t) = \langle \delta c(\mathbf{0}; 0, t) \delta c(\mathbf{r}; 0, t) \rangle, \quad (6)$$

and translational invariance has been taken into account ( $\rho = N/V$  denotes the mean density). The above equations show that  $\chi_4(t)$  measures the extent of spatial correlation between dynamical events between times 0 and  $t$  at different points of the system, i. e., the spatial extent of dynamically heterogeneous regions over a time span  $t$ .

The function  $\chi_4(t)$  has been measured by molecular dynamics, Brownian and Monte Carlo simulations in different liquids [14,28,29,76,163]. An example is shown in Fig. 11 for a Lennard-Jones liquid. The qualitative behaviour is similar in all cases [21,79,159]: as a function of time  $\chi_4(t)$  first increases, it has a peak on a timescale that tracks the structural relaxation timescale and then it decreases<sup>2</sup>. The peak value measures thus the volume on which the structural relaxation processes are correlated. It is found to increase when the temperature decreases and the dynamics slows down. By measuring directly  $G_4(\mathbf{r}; 0, t)$  it has also been checked that the increase of the peak of  $\chi_4(t)$  corresponds, as expected, to a growing dynamic lengthscale  $\xi$  [14,21,28], although these measurements are much harder in computer simulations, because very large systems need to be simulated to determine  $\xi$  unambiguously. Note that if the dynamically correlated regions were compact, the peak of  $\chi_4$  would be proportional to  $\xi^3$  in three dimensions, directly relating  $\chi_4$  measurements to that of the relevant lengthscale of DH.

These results are also relevant because many theories of the glass transition assume or predict, in a way or another, that the dynamics slows down because there are increasingly large regions on which particles have to relax in

<sup>2</sup>The decrease at long times constitutes a major difference with spin glasses. In a spin glass,  $\chi_4$  would be a monotonically increasing function of time whose long-time limit coincides with the static spin glass susceptibility. Physically, the difference is that spin glasses develop long-range static amorphous order while structural glasses do not or, at least, in a different and more subtle way.



**Glasses and Aging: A Statistical Mechanics Perspective, Figure 11** Time dependence of  $\chi_4(t)$  quantifying the spontaneous fluctuations of the intermediate scattering function in a Lennard-Jones supercooled liquid. For each temperature,  $\chi_4(t)$  has a maximum, which shifts to larger times and has a larger value when  $T$  is decreased, revealing the increasing lengthscale of dynamic heterogeneity in supercooled liquids approaching the glass transition

a correlated or cooperative way. However, this lengthscale remained elusive for a long time. Measures of the spatial extent of dynamic heterogeneity, in particular  $\chi_4(t)$  and  $G_4(\mathbf{r}; 0, t)$ , seem to provide the long-sought evidence of this phenomenon. This in turn suggests that the glass transition is indeed a critical phenomenon characterized by growing timescales and lengthscales. A clear and conclusive understanding of the relationship between the lengthscale obtained from  $G_4(\mathbf{r}; 0, t)$  and the relaxation timescale is still the focus of an intense research activity.

One major issue is that obtaining information on the behaviour of  $\chi_4(t)$  and  $G_4(\mathbf{r}; 0, t)$  from experiments is difficult. Such measurements are necessary because numerical simulations can only be performed rather far from  $T_g$ , see Sect. “Numerical simulations”. Up to now, direct experimental measurements of  $\chi_4(t)$  have been restricted to colloidal [166] and granular materials [65,110] close to the jamming transition, because dynamics is more easily spatially resolved in those cases. Unfortunately, similar measurements are currently not available in molecular liquids.

Recently, an approach based on fluctuation-dissipation relations and rigorous inequalities has been developed in order to overcome this difficulty [20,21,22]. The main idea is to obtain a rigorous lower bound on  $\chi_4(t)$  using the Cauchy–Schwarz inequality  $\langle \delta H(0)\delta C(0, t) \rangle^2 \leq \langle \delta H(0)^2 \rangle \langle \delta C(0, t)^2 \rangle$ , where  $H(t)$  denotes the enthalpy at time  $t$ . By using fluctuation-dissipation relations the previous inequality can be rewritten as [20]

$$\chi_4(t) \geq \frac{k_B T^2}{c_P} [\chi_T(t)]^2, \quad (7)$$

where the multi-point response function  $\chi_T(t)$  is defined by

$$\chi_T(t) = \left. \frac{\partial F(t)}{\partial T} \right|_{N,P} = \frac{N}{k_B T^2} \langle \delta H(0)\delta C(0, t) \rangle.$$

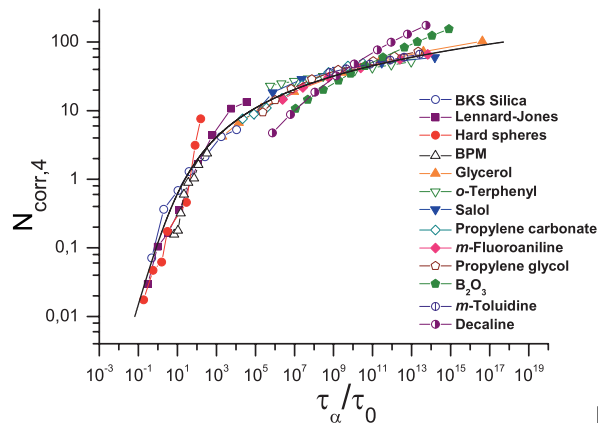
In this way, the experimentally accessible response  $\chi_T(t)$  which quantifies the sensitivity of average correlation functions  $F(t)$  to an infinitesimal temperature change, can be used in Eq. (7) to yield a lower bound on  $\chi_4(t)$ . Moreover, detailed numerical simulations and theoretical arguments [21,22] strongly suggest that the right hand side of (7) actually provides a good estimation of  $\chi_4(t)$ , not just a lower bound.

Using this method, Dalle-Ferrier et al. [63] have been able to obtain the evolution of the peak value of  $\chi_4$  for many different glass-formers in the entire supercooled regime. In Fig. 12 we show some of these results as a function of the relaxation timescale. The value on the y-axis, the peak of  $\chi_4$ , is a proxy for the number of molecules,  $N_{\text{corr},4}$  that have to evolve in a correlated way in order to relax the structure of the liquid. Note that  $\chi_4$  is expected to be equal to  $N_{\text{corr},4}$ , up to a proportionality constant which is not known from experiments, probably explaining why the high temperature values of  $N_{\text{corr},4}$  are smaller than one. Figure 12 also indicates that  $N_{\text{corr},4}$  grows faster when  $\tau_\alpha$  is not very large, close to the onset of slow dynamics, and a power law relationship between  $N_{\text{corr},4}$  and  $\tau_\alpha$  is good in this regime ( $\tau_\alpha/\tau_0 < 10^4$ ). The growth of  $N_{\text{corr},4}$  becomes much slower closer to  $T_g$ . A change of 6 decades in time corresponds to a mere increase of a factor about 4 of  $N_{\text{corr},4}$ , suggesting logarithmic rather than power law growth of dynamic correlations. This is in agreement with several theories of the glass transition which are based on activated dynamic scaling [85,155,171].

Understanding quantitatively this relation between timescales and lengthscales is one of the main recent topics addressed in theories of the glass transition, see Sect. “Some theory and models”. Furthermore, numerical works are also devoted to characterizing better the geometry of the dynamically heterogeneous regions [7,69].

### Some Theory and Models

We now present some theoretical approaches to the glass transition. It is impossible to cover all of them in a brief review, simply because there are way too many of them, perhaps the clearest indication that the glass transition remains an open problem. We choose to present approaches that are keystones and have a solid statistical mechanics basis. Loosely speaking, they have an Hamiltonian, can be simulated numerically, or studied analytically with statis-



**Glasses and Aging: A Statistical Mechanics Perspective, Figure 12** Universal dynamic scaling relation between number of dynamically correlated particles,  $N_{\text{corr},4}$ , and relaxation timescale,  $\tau_\alpha$ , for a number of glass-formers [63], determined using Eq. (7)

tical tools. Of course, the choice of Hamiltonians is crucial and contains very important assumptions about the nature of the glass transition. All these approaches have given rise to unexpected results. One finds more in them than what was supposed at the beginning, which leads to new, testable predictions. Furthermore, with models that are precise enough, one can test (and hopefully falsify!) these approaches by working out all their predictions in great detail, and comparing the outcome to experimental data. This is not possible with ‘physical pictures’, or simpler approaches of the problem which we have therefore avoided.

Before going into the models, we would like to state the few important questions that face theoreticians.

- Why do the relaxation time and the viscosity increase when  $T_g$  is approached? Why is this growth super-Arrhenius?
- Can one understand and describe quantitatively the average dynamical behaviour of supercooled liquids, in particular broad relaxation spectra, non-exponential behaviour, and their evolution with fragility?
- Is there a relation between kinetics and thermodynamics (like  $T_0 \simeq T_K$ ), and why?
- Can one understand and describe quantitatively the spatio-temporal fluctuations of the dynamics? How and why are these fluctuations related to the dynamic slowing down?
- Is the glass transition a collective phenomenon? If yes, of which kind? Is there a finite temperature or zero temperature ideal glass transition? In this case, is the transition of static or purely dynamic origin?

- Is there a geometric, real space explanation for the dynamic slowing down that takes into account molecular degrees of freedom?

The glass transition appears as a kind of ‘intermediate coupling’ problem, since for instance typical growing length-scales are found to be at most a few tens of particle large close to  $T_g$ . It would therefore be difficult to recognize the correct theory even if one bumped into it. To obtain quantitative, testable predictions, one must therefore be able to work out also preasymptotic effects. This is particularly difficult, especially in cases where the asymptotic theory itself has not satisfactorily been worked out. As a consequence, at this time, theories can only be judged by their overall predictive power and their theoretical consistency.

### Cooperativity, Chaotic Energy Landscapes and Random First Order Theory

In the last two decades, three *independent* lines of research approaches, Adam–Gibbs theory [2], mode-coupling theory [94] and spin glass theory [137], have merged to produce a theoretical ensemble that now goes under the name of Random First Order Theory (RFOT), a terminology introduced by Kirkpatrick, Thirumalai and Wolynes [111] who also played a major role in its development. Instead of following the rambling development of history, we summarize it in a more modern and unified way.

A key ingredient of RFOT is the existence of a chaotic or complex free energy landscape and its evolution with temperature and/or density. Analysing it in a controlled way for three dimensional interacting particles system is of course an impossible task. This can be achieved, however, in simplified models or using mean-field approximation, that have therefore played a crucial role in the development of RFOT.

A first, concrete example is given by ‘lattice glass models’ [37]. These are models containing hard particles sitting on the sites of a lattice. The Hamiltonian is infinite if there is more than one particle on a site or if the number of occupied neighbors of an occupied site is larger than a parameter,  $m$ , but the Hamiltonian is zero otherwise. Tuning the parameter  $m$ , or changing the type of lattice, in particular its connectivity, yields different models. Lattice glasses are constructed as simple statmech models to study the glassiness of hard sphere systems. The constraint on the number of occupied neighbors mimicks the geometric frustration [139] encountered when trying to pack hard spheres in three dimensions. Other models, which have a finite energy and, hence, are closer to molecular glass-formers, can be also constructed [131]. These models can

1092 be solved exactly on a Bethe lattice <sup>3</sup>, which reveals an as-  
 1093 tonishing physical behaviour [147]. In particular their free  
 1094 energy landscape can be analyzed in full details and turns  
 1095 out to have the properties that are also found in several  
 1096 ‘generalized spin glasses’.

1097 Probably the most studied example of such spin glasses  
 1098 is the  $p$ -spin model, defined by the Hamiltonian [93]

$$1099 \quad H = - \sum_{i_1, \dots, i_p} J_{i_1, \dots, i_p} S_{i_1} \dots S_{i_p}, \quad (8)$$

1100 where the  $S_i$ s are Ising or spherical spins,  $p > 2$  and  
 1101  $J_{i_1, \dots, i_p}$  quenched random couplings with zero mean vari-  
 1102 ance  $p!/(2N^{p-1})$ .

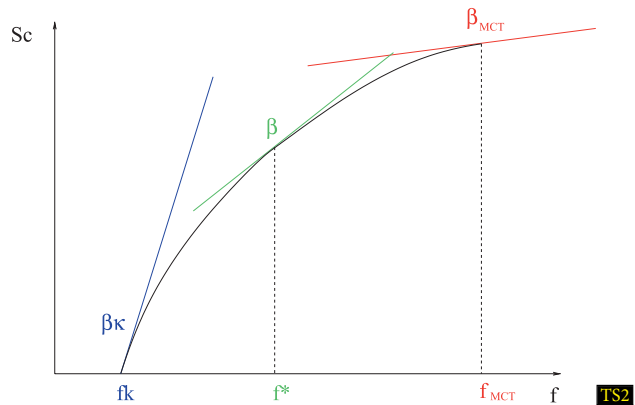
1103 All these models (lattice glasses, their finite energy gen-  
 1104 eralizations and their quenched disorder counterparts) be-  
 1105 long the class of one-step replica symmetry breaking sys-  
 1106 tems [137]. This makes reference to the ansatz that is  
 1107 needed [93]. when replica techniques are used to compute  
 1108 the thermodynamic behaviour of the model in Eq. (8).  
 1109 This corresponds to the universality class of chaotic (or  
 1110 random) free energy landscapes, as we now explain.

1111 The free energy landscape of these systems is ‘rugged’,  
 1112 characterized by many minima and saddle points. Actu-  
 1113 ally, the number of stationary points is so large that  
 1114 in order to count them one has to introduce an en-  
 1115 tropy, called configurational entropy or complexity,  $s_c =$   
 1116  $1/N \log \mathcal{N}(f)$ , where  $\mathcal{N}(f)$  is the number of stationary  
 1117 points with a given free energy density  $f$ . The density pro-  
 1118 file corresponding to one given minimum is amorphous  
 1119 and lacks any type of periodic long-range order, and differ-  
 1120 ent mimima are very different. Defining a similarity mea-  
 1121 sure between them, an ‘overlap’, one typically finds that  
 1122 two minima with the same free energy  $f$  have zero overlap.  
 1123 The typical shape of the configurational entropy as a func-  
 1124 tion of  $f$  is plotted in Fig 13.

1125 At high temperature, there is typically a single mini-  
 1126 mum, the high temperature liquid state. There is a tem-  
 1127 perature below which an exponentially large (in the sys-  
 1128 tem size) number of minima appears. Within mean-field  
 1129 models, corresponding to Bethe or completely connected  
 1130 lattices, these minima correspond to macroscopic physical  
 1131 states analogous to the periodic minimum corresponding to  
 1132 the crystal <sup>4</sup>. Once the system is in one of these states it re-  
 1133 mains trapped in it forever, since barriers separating states

<sup>3</sup>In order to have a well-defined thermodynamics, Bethe lattices are generated as random graphs with fixed connectivity, also called random regular graphs.

<sup>4</sup>There is of course no crystal state in disordered systems such as in Eq. (8). In the case of lattice glass models, there is a crystal phase but it can disappear depending whether the Bethe lattice is a Cayley tree or a random regular graph.



**Glasses and Aging: A Statistical Mechanics Perspective, Figure 13**  
 Typical shape of the configurational entropy,  $s_c$ , as a function of free energy density,  $f$  in the range  $T_K < T < T_{MCT}$  for random first order landscapes. A graphic solution of Eq. (10) is obtained by finding the value of  $f$  at which the slope of the curve is  $\beta$ . Note that  $s_c$  is also a function of temperature, so this curve in fact changes with  $T$

1134 diverge with the system size. However, when transposed to  
 1135 finite dimensional systems, these states become metastable  
 1136 and have a finite lifetime. As a consequence, in order to  
 1137 compute thermodynamic properties, one has to sum over  
 1138 all of them using the Boltzmann weight  $\exp(-\beta N f_\alpha)$  for  
 1139 each state  $\alpha$  [135]:

$$1140 \quad Z = \sum_{\alpha} e^{-\beta N f_\alpha} = \int df \exp[N s_c(f; T)] e^{-\beta N f}, \quad (9)$$

1141 where  $\beta = 1/(K_B T)$ . Evaluating this sum by saddle point  
 1142 method yields three regimes. At high temperature,  $T >$   
 1143  $T_{MCT}$ , the liquid corresponding to a flat density profile  
 1144 dominates the sum. The landscape is simple and has a sin-  
 1145 gular minimum. This is followed by an intermediate tem-  
 1146 perature regime,  $T_K < T < T_{MCT}$ , where the sum is do-  
 1147 minated by all terms with free energy density satisfying

$$1148 \quad \left. \frac{\partial s_c(f, T)}{\partial f} \right|_{f=f^*} = \beta . \quad (10)$$

1149 There are many of them, the logarithm of their number be-  
 1150 ing given by  $N s_c(f^*, T)$ , see Fig. 13 for a graphical solution  
 1151 of Eq. (10). Upon decreasing the temperature,  $s_c(f^*, T)$   
 1152 decreases until a temperature,  $T_K$ , below which the sum  
 1153 in Eq. (9) becomes dominated by only few terms corre-  
 1154 sponding to states with free energy density  $f_K$  given by  
 1155  $s_c(f_K, T) = 0$ , see Fig. 13. The entropy in the interme-  
 1156 diate temperature range above  $T_K$  has two contributions:  
 1157 the one counting the number of minima, given by  $s_c$ , and  
 1158 the intra-state entropy,  $s_{in}$ , counting the number config-

1159 urations inside each state. At  $T_K$ , the configurational en- 1208  
 1160 tropy vanishes,  $s_c(T_K) = 0$ . As a consequence the specific 1209  
 1161 heat undergoes a jump towards a smaller value across  $T_K$ , 1210  
 1162 an exact realization of the ‘entropy vanishing’ mechanism 1211  
 1163 conjectured by Kauzmann [108]. 1212

1164 Let us discuss the dynamical behaviour which results 1213  
 1165 from the above analysis. We have already mentioned that 1214  
 1166 relaxation processes do not occur below  $T_{MCT}$  because 1215  
 1167 states have an infinite lifetime. The stability of these states 1216  
 1168 can be analyzed by computing the free energy Hessian in 1217  
 1169 the minima [48]. One finds that states become more fragile 1218  
 1170 when  $T \rightarrow T_{MCT}^-$ , are marginally stable at  $T = T_{MCT}$ , un- 1219  
 1171 stable for  $T > T_{MCT}$ . The dynamics of these models can be 1220  
 1172 analyzed exactly [58]. Coming from high temperature, the 1221  
 1173 dynamics slows down and the relaxation time diverges at 1222  
 1174  $T_{MCT}$  in a power law manner, 1223

$$1175 \quad \tau_\alpha \sim \frac{1}{(T - T_{MCT})^\gamma}, \quad (11) \quad 1224$$

1176 where  $\gamma$  is a critical exponent. The physical reason is the 1225  
 1177 incipient stable states that appear close to  $T_{MCT}$ . The closer 1226  
 1178 the temperature is to  $T_{MCT}$ , the longer it takes to find an 1227  
 1179 unstable direction to relax. 1228

1180 Amazingly, the dynamical transition that appears up- 1229  
 1181 on approaching  $T_{MCT}$  in random first order landscapes 1230  
 1182 is completely analogous to the one predicted to occur 1231  
 1183 in supercooled liquids by the Mode-Coupling Theory 1232  
 1184 of the glass transition, and developed independently by 1233  
 1185 Leuthesser, Bengtzelius, Götze, Sjölander and coworkers 1234  
 1186 [94]. Actually, MCT can be considered as an approx- 1235  
 1187 imation which becomes controlled and exact for these 1236  
 1188 mean-field models. Originally, MCT was developed using 1237  
 1189 projector operator formalism [13,122] and field-theory 1238  
 1190 methods [64] to yield closed integro-differential equations 1239  
 1191 for the dynamical structure factor in supercooled liquids. 1240  
 1192 These approaches were recently generalized [34,36] to deal 1241  
 1193 with dynamic heterogeneity and make predictions for the 1242  
 1194 multi-point susceptibilities and correlation functions dis- 1243  
 1195 cussed in Sect. “Dynamic heterogeneity”. Within MCT, 1244  
 1196 the relaxation timescale diverges in a power law fashion 1245  
 1197 at  $T_{MCT}$ , as in Eq. (11). This divergence is accompanied by 1246  
 1198 critical behaviour that appears both in space (long range 1247  
 1199 spatial dynamic correlations), and in time (power laws in 1248  
 1200 time). 1249

1201 Comparing Eqs. (1) and (11) makes it clear that MCT 1250  
 1202 cannot be used to describe viscosity data close to  $T_g$  since it 1251  
 1203 does not predict activated behaviour. It is now recognized 1252  
 1204 that an MCT transition at  $T_{MCT}$  does not occur in real 1253  
 1205 materials, so that  $T_{MCT}$  is, at best, a dynamical crossover. 1254  
 1206 A central advantage of MCT, compared to many other the- 1255  
 1207 ories (this includes the  $T \approx T_K$  regime of RFOT itself) 1256

1208 is that it can yield quantitative predictions from micro- 1209  
 1210 scopic input obtained for a particular material. As such 1211  
 1212 it has been applied to yield predictions for scores of dif- 1213  
 1214 ferent systems that can be directly confronted to exper- 1214  
 1215 imental or numerical measurements. A major drawback 1215  
 1216 is the freedom offered by the ‘crossover’ nature of the 1216  
 1217 MCT transition, so that ‘negative’ results can often be at- 1217  
 1218 tributed to corrections to asymptotic predictions rather 1218  
 1219 than deficiencies of the theory itself. Nevertheless, MCT 1219  
 1220 has proven to be useful and continues to be developed, ap- 1220  
 1221 plied and generalized to study many different physical sit- 1221  
 1222 uations [94], including aging systems and non-linear rhe- 1222  
 1223 ology of glassy materials [18,83,134], see Sect. “Aging and 1223  
 1224 off-equilibrium”. 1224

1225 What happens below  $T_{MCT}$  in finite dimensional sys- 1225  
 1226 tem if the relaxation time does not diverge as predicted in 1226  
 1227 Eq. (11)? Why is the transition avoided? In fact, the plethora 1227  
 1228 of states that one finds in mean-field are expected to be- 1228  
 1229 come (at best) metastable in finite dimension, with a finite 1229  
 1230 lifetime, even below  $T_{MCT}$ . What is their typical lifetime, 1230  
 1231 and how these metastable states are related to the struc- 1231  
 1232 tural relaxation are issues that still await for a complete 1232  
 1233 microscopic analysis. 1233

1234 There exist, however, phenomenological arguments 1234  
 1235 [38,112,171], backed by microscopic computations [71, 1235  
 1236 80] that yield a possible solution dubbed ‘mosaic state’ 1236  
 1237 by Kirkpatrick, Thirumalai and Wolynes [112]. Schemat- 1237  
 1238 ically, the mosaic picture states that, in the regime  $T_K < 1238  
 1239 T < T_{MCT}$ , the liquid is composed of domains of linear 1239  
 1240 size  $\xi$ . Inside each domain, the system is in one of 1240  
 1241 the mean-field states. The length of the domains is fixed 1241  
 1242 by a competition between energy and configurational en- 1242  
 1243 tropy. A state in a finite but large region of linear size  $l$  can 1243  
 1244 be selected by appropriate boundary conditions that de- 1244  
 1245 crease its free energy by an amount which scales as  $\Upsilon l^\theta$  1245  
 1246 with  $\theta \leq 2$ . On the other hand, the system can gain en- 1246  
 1247 tropy, which scales as  $s_c l^3$ , if it visits the other numerous 1247  
 1248 states. Entropy obviously gains on large lengthscales, the 1248  
 1249 crossover length  $\xi$  being obtained by balancing the two 1249  
 1250 terms, 1250

$$1248 \quad \xi = \left( \frac{\Upsilon}{T s_c(T)} \right)^{1/(3-\theta)}. \quad (12) \quad 1248$$

1249 In this scenario, the configurational entropy on scales 1249  
 1250 smaller than  $\xi$  is too small to stir the configurations effi- 1250  
 1251 ciently and win over the dynamically generated pinning 1251  
 1252 field due to the environment, while ergodicity is restored 1252  
 1253 at larger scale. Hence, the relaxation time of the system is 1253  
 1254 the relaxation time,  $\tau(\xi)$ , of a finite size regions of the sys- 1254  
 1255 tem. Barriers are finite, unlike in the mean-field treatment. 1255  
 1256 Smaller length scales are faster but unable to decorrelate, 1256



1257 whereas larger scales are orders of magnitude slower. As- 1303  
 1258 suming thermal activation over energy barriers which are 1304  
 1259 supposed to grow with size as  $\xi^\psi$ , one predicts finally, us- 1305  
 1260 ing Eq. (12), that [38] 1306

$$1261 \log\left(\frac{\tau_\alpha}{\tau_0}\right) = c \frac{\gamma}{k_B T} \left(\frac{\gamma}{T s_c(T)}\right)^{\psi/(3-\theta)}, \quad (13) \quad 1307$$

1262 where  $c$  is a constant. 1308

1263 The above argument is rather generic and there- 1309  
 1264 fore not very predictive. Recent microscopic computa- 1310  
 1265 tions [71,80] aimed at putting these phenomenological 1311  
 1266 arguments on a firmer basis and computing the exponents 1312  
 1267  $\theta$  and  $\psi$ . The results are unfortunately not yet conclusive be- 1313  
 1268 cause they involve replica calculations with uncontrolled 1314  
 1269 assumptions, but they do confirm the phenomenological 1315  
 1270 scenario presented above and suggest that  $\theta = 2$ . Some 1316  
 1271 other phenomenological arguments suggest the value of 1317  
 1272  $\theta = 3/2$  [112]. There are no computation available for  $\psi$ , 1318  
 1273 only the suggestion that  $\psi = \theta$  [112]. 1319

1274 Note that using the value  $\theta = 3/2$  with  $\theta = \psi$  simpli- 1320  
 1275 fies Eq. (13) into a form that is well-known experimentally 1321  
 1276 and relates  $\log \tau_\alpha$  directly to  $1/S_c$ , which is the celebrated 1322  
 1277 Adam–Gibbs relation [2] between relaxation time and 1323  
 1278 configurational entropy that is in rather good quantitative 1324  
 1279 agreement with many experimental results [5,96,105]. The 1325  
 1280 Random First Order Theory can be considered, therefore, 1326  
 1281 as a microscopic theory that reformulates and generalizes 1327  
 1282 the Adam–Gibbs mechanism. Furthermore, using the fact 1328  
 1283 that the configurational entropy vanishes linearly at  $T_K$  1329  
 1284 one predicts also a VFT divergence of the relaxation time 1330  
 1285 as in Eq. (1), with the identification that 1331

$$1286 T_0 = T_K. \quad (14) \quad 1332$$

1287 The equality (14) between two temperatures that are 1333  
 1288 commonly used in the description of experimental data 1334  
 1289 certainly constitutes a central achievement of RFOT since 1335  
 1290 it accounts for the empirical relation found between the 1336  
 1291 kinetics and the thermodynamics of supercooled liquids. 1337  
 1292 Furthermore RFOT naturally contains MCT, which can be 1338  
 1293 used to describe the first decades of the dynamical slow- 1339  
 1294 ing down, while the spin glass side of RFOT qualitatively 1340  
 1295 explains the dynamics in terms of the peculiar features of 1341  
 1296 the free energy landscape that have been detailed above. 1342  
 1297 Dynamics first slows down because there appear incipi- 1343  
 1298 ent metastable states, and once this metastable states are 1344  
 1299 formed, the dynamics becomes dominated by the ther- 1345  
 1300 mally activated barrier crossing from one metastable state 1346  
 1301 to another, which is consistent with the relation between 1347  
 1302 dynamical correlation length and timescale discussed in 1348

1303 Sect. “Dynamic heterogeneity”. Quite importantly, micro- 1304  
 1305 scopic computations of  $T_{MCT}$  and  $T_0$  for realistic mod- 1306  
 1307 els of liquids are possible [136]. Remarkably, the jamming 1308  
 1309 transition of hard spheres systems has been also studied 1309  
 1310 with these techniques and a clear connection with the glass 1310  
 1311 transition has emerged within RFOT [143]. This quantita- 1311  
 1312 tive “side” of RFOT is a most desirable feature, even if the 1312  
 1313 results are not always quantitatively accurate [54,138,156]. 1313

1314 Probably the most serious weakness of the RFOT con- 1314  
 1315 struction is that the theory, although worked out in full 1315  
 1316 details within mean-field models, has remained elusive for 1316  
 1317 finite dimensional systems, for which it has a highly spec- 1317  
 1318 ulative flavour. Worrying is the fact that no simple three- 1318  
 1319 dimensional glassy model, let alone interacting particles in 1319  
 1320 the continuum, has been discovered, for which this theo- 1320  
 1321 ry has been shown to apply, and the entropy driven nu- 1321  
 1322 cleation theory that leads to the VFT law is not under- 1322  
 1323 stood completely. Although the ultimate consequences of 1323  
 1324 the theory are sometimes in very good agreement with ex- 1324  
 1325 periments, as Eq. (14), one should not conclude that RFOT 1325  
 1326 is correct. In fact direct tests of the mosaic state picture are 1326  
 1327 rare, and rather inconclusive [49]. One can hope that in 1327  
 1328 the next few years, joint theoretical and experimental ef- 1328  
 1329 forts will drive RFOT into a corner, to a point where it can 1329  
 1330 be decided whether it is truly a valid theory for the glass 1330  
 1331 transition. 1331

### 1329 Free Volume, Defects, and Facilitated Models 1332

1330 In this subsection we motivate and briefly summarize 1331  
 1331 studies of a different family of statistical mechanics models 1332  
 1332 that turns out to yield a rich variety of physical behaviours. 1333  
 1333 Their starting point are physical assumptions that might 1334  
 1334 seem similar to the models described in Sect. “Coopera- 1335  
 1335 tivity, chaotic energy landscapes and Random First Order 1336  
 1336 Theory”, but the outcome yields a different physical ex- 1337  
 1337 planation of the glass transition. Although the two theo- 1338  
 1338 retical approaches cannot be simultaneously correct, they 1339  
 1339 both have been influential and very instructive in order to 1340  
 1340 develop a theoretical understanding of glassy phenomena. 1341  
 1341 Furthermore, despite the ‘great unification’ phase diagram 1342  
 1342 in Fig. 4, it could be that glass and jamming transitions in 1343  
 1343 colloids, granular media and glass-formers have a different 1344  
 1344 nature, so that different theories could apply to different 1345  
 1345 phenomena. 1346

1346 As in Sect. “Cooperativity, chaotic energy landscapes 1347  
 1347 and Random First Order Theory”, we start from the pack- 1348  
 1348 ing considerations that are more appropriate for hard 1349  
 1349 spheres systems. We follow first Kob and Andersen [115] 1350  
 1350 and again use a lattice gas description of the physics and 1351  
 1351 work on a three dimensional cubic lattice. As in a hard 1352

1352 sphere system, we assume no interaction between parti-  
 1353 cles beyond the hard-core constraint that the occupation  
 1354 number  $n_i$  at site  $i$  is at most equal to 1,

$$1355 \quad H[\{n_i\}] = 0, \quad n_i = 0, 1. \quad (15)$$

1356 Contrary to the lattice glass model presented above, all  
 1357 configurations respecting the hard-core constraint are al-  
 1358 lowed and are equally probable. Geometric frustration is  
 1359 instead introduced at the level of the kinetic rules, that are  
 1360 defined as constrained local moves. Namely, a particle can  
 1361 jump to a nearest neighbor site only if that site is empty (to  
 1362 satisfy the hard-core constraint), but, additionnally, only  
 1363 if the sites occupied before and after the move have less  
 1364 than  $m$  neighbors,  $m$  being an adjustable parameter, which  
 1365 Kob and Andersen choose as  $m = 4$  for  $d = 3$  ( $m = 6$  cor-  
 1366 responds to the unconstrained lattice gas). The model cap-  
 1367 tures the idea that if the liquid is locally very dense, no  
 1368 movement is possible while regions with low density move  
 1369 more easily.

1370 Of course, such kinetically constrained lattice gases  
 1371 have been studied in various spatial dimensions, for dif-  
 1372 ferent values of  $m$ , for different constraints, or even dif-  
 1373 ferent lattice geometries [146]. They can be thought of as  
 1374 models capturing the idea of a ‘cage’ effect in a strict sense,  
 1375 utilizing the notion that a particle with a dense neighbor  
 1376 shell cannot diffuse. Although the cage seems a purely lo-  
 1377 cal concept, it turns out that diffusion in constrained lat-  
 1378 tice gases arises from cooperative rearrangments, so that  
 1379 slow dynamics can be directly shown to be driven by  
 1380 the growth of dynamic lengthscales for these cooperative  
 1381 moves [77,141,157]. This strongly suggests that such co-  
 1382 operative moves are most probably at work also in real liq-  
 1383 uids.

1384 In this lattice gas picture, the connection with liquid  
 1385 is not obvious because density (‘free volume’), rather than  
 1386 temperature controls the dynamics. Thermal models with  
 1387 similar features can in fact be defined along the follow-  
 1388 ing lines. In a liquid, low temperature implies a very small  
 1389 probability to find a location with enough free volume to  
 1390 move. The idea of a small concentration of ‘hot spots’ is  
 1391 in fact reminiscent of another picture of the glass transi-  
 1392 tion based on the idea of ‘defects’ which is captured by  
 1393 the defect model proposed by Glarum [87] in the 60’s,  
 1394 where relaxation proceeds via the diffusion of a low con-  
 1395 centration of independent defects. In the mid-80’s, using  
 1396 the conjugated ideas of kinetic constraints and rare defects,  
 1397 Fredrickson and Andersen defined a family of kinetic Ising  
 1398 models for the glass transition [81]. They study an assem-

bly of non-interacting spins,

$$1399 \quad H[\{n_i\}] = \sum_{i=1}^N n_i, \quad n_i = 0, 1, \quad (16) \quad 1400$$

1401 where  $n_i = 1$  represent the defects, whose concentration  
 1402 becomes exponentially small at low temperature,  $\langle n_i \rangle \approx$   
 1403  $\exp(-1/T)$ . As for the Kob–Andersen lattice gas, the non-  
 1404 trivial ingredient lies in the chosen rates for the transition  
 1405 between states. The kinetic rules stipulate that a transition  
 1406 at site  $i$  can happen with a usual Glauber rate, but only if  
 1407 site  $i$  is surrounded by at least  $k$  defects ( $k = 0$  corresponds  
 1408 to the unconstrained limit). Again, one can easily imagine  
 1409 studying such models in different spatial dimensions, on  
 1410 different lattices, and with slightly different kinetic rules,  
 1411 yielding a large number of possible behaviours [125,146].  
 1412 The similarity between those spin facilitated models and  
 1413 the kinetically constrained lattice gases is striking. Alto-  
 1414 gether, they form a large family of models generically  
 1415 called kinetically constrained models (KCMs) [146].

1416 The connection between KCMs and the much older  
 1417 concept of free volume is obvious from our presenta-  
 1418 tion. Free volume models are among the most widely  
 1419 used models to analyze experimental data, especially in  
 1420 polymeric systems. They have been thoroughly reviewed  
 1421 before [53,66], and the main prediction is that dynamic  
 1422 slowing down occurs because the free volume available  
 1423 to each particle,  $v_f$ , vanishes at some temperature  $T_0$   
 1424 as  $v_f \approx \alpha(T - T_0)$ , a relation which connects volume to  
 1425 temperature. Statistical arguments then relate relaxation  
 1426 timescales to free volume assuming that movement is possi-  
 1427 ble if locally there is ‘enough’ free volume available, more  
 1428 than a typical value  $v_0$ . This is clearly reminiscent of the  
 1429 above idea of a kinetic constraint for local moves in lattice  
 1430 gases. An appealing VFT divergence is then predicted:

$$1431 \quad \frac{\tau_\alpha}{\tau_0} \sim \exp\left(\gamma \frac{v_0}{v_f}\right) \sim \exp\left(\frac{\gamma v_0/\alpha}{[T - T_0]^\mu}\right), \quad (17)$$

1432 where  $\gamma$  is a numerical factor and  $\mu = 1$ . Predictions  
 1433 such as Eq. (17) justify the wide use of free volume ap-  
 1434 proaches, despite the many (justified) criticisms that have  
 1435 been raised.

1436 Initially it was suggested that KCMs would similarly  
 1437 display finite temperature or finite density dynamic tran-  
 1438 sitions similar to the one predicted by the mode-coupling  
 1439 theory of supercooled liquids [81], but it was soon real-  
 1440 ized [46,82] that most KCMs do not display such singu-  
 1441 larity, and timescales in fact only diverge in the limit of  
 1442 zero temperature ( $T = 0$ ) or maximal density ( $\rho = 1$ ). Re-  
 1443 cently, models displaying a  $T_c > 0$  or  $\rho_c < 1$  transition

1444 have been introduced and analyzed [158]. They provide  
 1445 a microscopic realization, based on well-defined statistical  
 1446 mechanics models, of the glass transition predicted by free  
 1447 volume arguments. Their relaxation timescale diverges  
 1448 with a VFT-like form but with an exponent  $\mu \simeq 0.64$ . Un-  
 1449 derstanding their universality classes and how general is  
 1450 the mechanism leading to the transition is still an open  
 1451 problem.

1452 Extensive studies have shown that KCMs have a mac-  
 1453 roscopic behaviour which resembles the phenomenology  
 1454 of supercooled liquids, displaying in particular Arrhenius  
 1455 or super-Arrhenius increase of relaxation timescales on  
 1456 decreasing the temperature and non-exponential relax-  
 1457 ation functions at equilibrium [146]. Early studies also  
 1458 demonstrated that, when suddenly quenched to very low  
 1459 temperatures, the subsequent non-equilibrium aging dy-  
 1460 namics of the models compares well with experimental ob-  
 1461 servations on aging liquids [82]. Moreover, the many pos-  
 1462 sibilities to define the models mean that they might exhibit  
 1463 a broad variety of possible behaviours. This is both a pos-  
 1464 itive and a negative aspect: on the one hand one can ex-  
 1465 plore various scenarii to describe glass transition phenom-  
 1466 ena, but on the other hand, one would like to be able to  
 1467 decide what particular model should be used if one wants  
 1468 to get a predictive quantitative description for a particular  
 1469 liquid. In fact, contrary to MCT, no microscopic calcula-  
 1470 tions have been performed using the framework of KCMs.  
 1471 Rather than predicting the quantitative behaviour of a ma-  
 1472 terial in all its microscopic details, it is perhaps more ap-  
 1473 propriate to use KCMs as theoretical tools to define con-  
 1474 cepts and obtain new ideas.

1475 It is precisely in this perspective that interest in KCMs  
 1476 continues to increase, in large part since it was realized  
 1477 that their dynamics is spatially heterogeneous [46,77,84],  
 1478 a central feature of supercooled liquids dynamics. It is only  
 1479 fair to say that in-depth studies of KCMs have greatly con-  
 1480 tributed to our theoretical understanding of the spatially  
 1481 heterogeneous dynamics in glass and jamming problems.  
 1482 Remarkably, virtually all the aspects related to dynamic  
 1483 heterogeneity mentioned in Sect. “Dynamic heterogene-  
 1484 ity” can be investigated and rationalized, at least qualita-  
 1485 tively, in terms of KCMs. The dynamics of these systems  
 1486 can be understood in terms of defects motion [146]. De-  
 1487 pending on the particular model, defects can diffuse or  
 1488 have a more complicated motion. Furthermore, they can  
 1489 simply be point-like, or ‘cooperative’ (formed by point-  
 1490 like defects moving in a cooperative way). A site can relax  
 1491 when it is visited by a defect. As a consequence, the het-  
 1492 erogeneous character of the dynamics is entirely encoded  
 1493 in the defect configuration and defect motion [84]. For in-  
 1494 stance, a snapshot similar to Fig. 7 in a KCM shows clus-

1495 ters which have relaxed within the time interval  $t$  [26,167].  
 1496 These are formed by all sites visited by a defect between  
 1497 0 and  $t$ . The other sites are instead frozen in their ini-  
 1498 tial state. In these models the dynamics slows down be-  
 1499 cause the defect concentration decreases. As a conse-  
 1500 quence, in the regime of slow dynamics there are few de-  
 1501 fects and strong dynamic heterogeneity. Detailed numer-  
 1502 ical and analytical studies have indeed shown that in these  
 1503 systems, non-exponential relaxations patterns do stem  
 1504 from a spatial, heterogeneous distribution of timescales,  
 1505 directly connected to a distribution of dynamic length-  
 1506 scales [84,103,141,157,158,167]. Decoupling phenomena  
 1507 appear in KCMs and can be shown to be very direct, quan-  
 1508 tifiable, consequences of the dynamic heterogeneity [106],  
 1509 which also deeply affects the process of self-diffusion in  
 1510 a system close to its glass transition [24]. More fundamen-  
 1511 tally, multi-point susceptibilities, multi-point spatial cor-  
 1512 relation functions such as the ones defined in Eqs. (3) and  
 1513 (6) can be studied in much greater detail than in molec-  
 1514 ular systems, to the point that scaling relations between  
 1515 timescales, lengthscales, and dynamic susceptibilities can  
 1516 be established [22,50,141,159,168]. This type of scaling be-  
 1517 haviour has been observed close to  $T = 0$  and  $\rho = 1$  in spin  
 1518 models and lattice gases without a transition<sup>5</sup>. These par-  
 1519 ticular points of the phase diagram have been shown, by  
 1520 various theoretical means, to correspond to true critical  
 1521 points where timescales and dynamic lengthscales diverge  
 1522 with well-defined critical laws [103,168]. Such ‘dynamic  
 1523 criticality’ is a useful concept because it implies the possi-  
 1524 bility that some universal behaviour emerges in the physics  
 1525 of supercooled liquids, precisely of the type observed in  
 1526 Fig. 12.

1527 A central criticism about the free volume approach,  
 1528 that is equally relevant for KCMs concerns the identi-  
 1529 fication, at the molecular level, of the vacancies (in lat-  
 1530 tice gases), mobility defects (in spin facilitated models), or  
 1531 free volume itself. Attempts to provide reasonable coarse-  
 1532 graining from molecular models with continuous degrees  
 1533 of freedom to lattice models with kinetic rules are so far  
 1534 very limited, and not really convincing [70,163]. On the  
 1535 other hand the proof that kinetic rules can emerge effec-  
 1536 tively and induce a slow dynamics has been obtained for  
 1537 simple lattice spin models [86], whose dynamics directly  
 1538 maps onto constrained models. Several examples are avail-  
 1539 able but here we only mention the simple case of the bidi-  
 1540 mensional plaquette model defined by a Hamiltonian of  
 1541 a  $p$ -spin type, but in two dimensions on a square lattice of

<sup>5</sup>A critical (different) behaviour is expected and predicted for models having a transition [158].

1542 linear size  $L$ ,

$$1543 \quad H = -J \sum_{i=1}^{L-1} \sum_{j=1}^{L-1} S_{i,j} S_{i+1,j} S_{i,j+1} S_{i+1,j+1}, \quad (18)$$

1544 where  $S_{i,j} = \pm 1$  is an Ising variable lying at node  $(i, j)$   
 1545 of the lattice. Contrary to KCMs, the Hamiltonian in  
 1546 Eq. (18) contains genuine interactions, which are no less  
 1547 (or no more) physical than  $p$ -spin models discussed in  
 1548 Sect. “Cooperativity, chaotic energy landscapes and Ran-  
 1549 dom First Order Theory”. Interestingly the dynamics of  
 1550 this system is (trivially) mapped onto that of a KCM by  
 1551 analyzing its behaviour in terms of plaquette variables,  
 1552  $p_{i,j} \equiv S_{i,j} S_{i+1,j} S_{i,j+1} S_{i+1,j+1}$ , such that the Hamiltonian  
 1553 becomes a non-interacting one,  $H = -J \sum_{i,j} p_{i,j}$ , as in  
 1554 Eq. (16). More interestingly, the analogy also applies to the  
 1555 dynamics [86]. The fundamental moves are spin-flips, but  
 1556 when a single spin is flipped the states of the four plaquet-  
 1557 tes surrounding that spin change. Considering the differ-  
 1558 ent types of moves, one quickly realizes that excited plaquet-  
 1559 tettes,  $p_{i,j} = +1$ , act as sources of mobility, since the en-  
 1560 ergetic barriers to spin flips are smaller in those regions.  
 1561 This observation allows to identify the excited plaquettes  
 1562 as defects, by analogy with KCMs. Spatially heterogeneous  
 1563 dynamics, diverging lengthscales accompanying diverg-  
 1564 ing timescales and scaling behaviour sufficiently close to  
 1565  $T = 0$  can be established by further analysis [101], provid-  
 1566 ing a simple, but concrete example, of how an interact-  
 1567 ing many body system might effectively behave as a model  
 1568 with kinetic constraints<sup>6</sup>.

1569 Another essential drawback of facilitated models is  
 1570 that among the microscopic ‘details’ thrown away to arrive  
 1571 at simple statmech models such as the ones in Eqs. (15)  
 1572 and (16), information on the thermodynamic behaviour  
 1573 of the liquids has totally disappeared. In particular, a pos-  
 1574 sible coincidence between VFT and Kauzmann tempera-  
 1575 tures,  $T_0$  and  $T_K$  is not expected, nor can the dynamics be  
 1576 deeply connected to thermodynamics, as in Adam–Gibbs  
 1577 relations. The thermodynamic behaviour of KCMs ap-  
 1578 pears different from the one of real glass-formers close to  
 1579  $T_g$  [35]. This is probably the point where KCMs and RFOT  
 1580 approaches differ more evidently. Even though the dy-  
 1581 namics of KCMs shares similarities with systems charac-  
 1582 terized with a complex energy landscape [25,169], thermo-  
 1583 dynamical behaviours are widely different in both cases, as  
 1584 has been recently highlighted in [102] by focusing on the  
 1585 concrete examples of plaquette models such as in Eq. (18).

<sup>6</sup>This type of plaquette models, and other spin models, were intro-  
 duced originally [123,149] to show how ultra-slow glassy dynamics  
 can emerge because of growing free energy barriers.

1586 Finally, when KCMs were first defined, they were ar-  
 1587 gued to display a dynamic transition of a nature very  
 1588 similar to the one predicted by MCT [81]. Although the  
 1589 claim has been proven wrong<sup>7</sup>, it bears some truth: both  
 1590 approaches basically focus on the kinetic aspects of the  
 1591 glass transition and they both predict the existence of  
 1592 some dynamic criticality with diverging lengthscales and  
 1593 timescales. This similarity is even deeper, since a mode-  
 1594 coupling singularity is truly present when (some) KCMs  
 1595 are studied on the Bethe lattice [157], but is ‘avoided’ when  
 1596 more realistic lattice geometries are considered. This un-  
 1597 derlies the similarity of these two approaches while em-  
 1598 phasizing further the mean-field character of the MCT ap-  
 1599 proach.

### 1600 Geometric Frustration, Avoided Criticality, 1601 and Coulomb Frustrated Theories

1602 In all of the above models, ‘real space’ was present in the  
 1603 sense that special attention was paid to different length-  
 1604 scales characterizing the physics of the models that were  
 1605 discussed. However, apart from the ‘packing models’ with  
 1606 hard-core interactions, no or very little attention was paid  
 1607 to the geometric structure of local arrangements in molec-  
 1608 ular liquids close to a glass transition. This slight ‘over-  
 1609 sight’ is generally justified using concepts such as ‘uni-  
 1610 versality’ or ‘simplicity’, meaning that one studies com-  
 1611 plex phenomena using simple models, a typical statisti-  
 1612 cal mechanics perspective. However, important questions  
 1613 remain: what is the liquid structure within mosaic states?  
 1614 How do different states differ? What is the geometric ori-  
 1615 gin of the defects invoked in KCMs? Are they similar to  
 1616 defects (disclinations, dislocations, vacancies, etc.) found  
 1617 in crystalline materials?

1618 There exists a line of research in this field which at-  
 1619 tempts to provide answers to these questions. It makes  
 1620 heavy use of the concept of geometric frustration. Broadly  
 1621 speaking, frustration refers to the impossibility of simul-  
 1622 taneously minimizing all the interaction terms in the en-  
 1623 ergy function of the system. Frustration might arise from  
 1624 quenched disorder (as in the spin glass models described  
 1625 above), but liquids have no quenched randomness. In that  
 1626 case, frustration has a purely geometric origin. It is at-  
 1627 tributed to a competition between a short-range tendency  
 1628 for the extension of a ‘locally preferred order’, and global  
 1629 constraints that prevent the periodic tiling of space with  
 1630 this local structure.

<sup>7</sup>Most KCMs do not have a finite temperature dynamical transi-  
 tion and the ones displaying a transition have critical properties dif-  
 ferent from MCT.

This can be illustrated by considering once more the packing problem of spheres in three dimensions. In that case, the locally preferred cluster of spheres is an icosahedron. However, the 5-fold rotational symmetry characteristic of icosahedral order is not compatible with translational symmetry, and formation of a periodic icosahedral crystal is impossible [75]. The geometric frustration that affects spheres in three dimensional Euclidean space can be relieved in curved space [139]. In Euclidian space, the system possesses topological defects (disclination lines), as the result of forcing the ideal icosahedral ordering into a ‘flat’ space. Nelson and coworkers have developed a solid theoretical framework based on this picture to suggest that the slowing down of supercooled liquids is due to the slow wandering of these topological defects [139], but their treatment remains so complex that few quantitative, explicit results have been obtained.

This picture of sphere packing disrupted by frustration has been further developed in simple statistical models characterized by geometric frustration, in a pure statistical mechanics approach [155]. To build such a model, one must be able to identify, then capture, the physics of geometric frustration. Considering a locally ordered domain of linear size  $L$ , Kivelson et al. [114] suggest that the corresponding free energy scales as

$$F(L, T) = \sigma(T)L^2 - \phi(T)L^3 + s(T)L^5, \quad (19)$$

The first two terms express the tendency of growing local preferred order and they represent respectively the energy cost of having an interface between 2 phases and a bulk free energy gain inside the domain. Geometric frustration is encoded in the third term which represents the strain free energy resulting from the frustration. The remarkable feature of Eq. (19) is the super-extensive scaling of the energy cost due to frustration which opposes the growth of local order. The elements in Eq. (19) can then be directly incorporated into ferromagnetic models where ‘magnetization’ represents the local order, ferromagnetic interactions the tendency to local ordering, and Coulombic anti-ferromagnetic interactions the opposite effect of the frustration. The following Hamiltonian possesses these minimal ingredients:

$$H = -J \sum_{\langle i, j \rangle} \mathbf{S}_i \cdot \mathbf{S}_j + K \sum_{i \neq j} \frac{\mathbf{S}_i \cdot \mathbf{S}_j}{|\mathbf{x}_i - \mathbf{x}_j|}, \quad (20)$$

where the spin  $\mathbf{S}_i$  occupies the site  $i$  at position  $\mathbf{x}_i$ . Such Coulomb frustrated models have been studied in great detail, using various approximations to study models for various space and spin dimensions [155].

The general picture is that the ferromagnetic transition occurring at  $T = T_c^0$  in the pure model with no frustration,  $K = 0$ , is either severely depressed to lower temperatures for  $K > 0$ , sometimes with a genuine discontinuity at  $K \rightarrow 0$ , yielding the concept of ‘avoided criticality’. For the simple case of Ising spins in  $d = 3$ , the situation is different since the second order transition becomes first order between a paramagnetic phase and a spatially modulated phase (stripes). For  $K > 0$  and  $T < T_c^0$  the system is described as a ‘mosaic’ of domains corresponding to some local order, whose size increases (but does not diverge!) when  $T$  decreases. Tarjus, Kivelson and co-workers clearly demonstrate that such a structuration into mesoscopic domains allows one to understand most of the fundamental phenomena occurring in supercooled liquids [155]. Their picture as a whole is very appealing because it directly addresses the physics in terms of the ‘real space’, and the presence of domains of course connects to ideas such as cooperativity, dynamic heterogeneity and spatial fluctuations, that directly explains, at least qualitatively, non-exponential relaxation, decoupling phenomena or super-Arrhenius increase of the viscosity. However, as for the RFOT mosaic picture, direct confirmations of this scenario are rare [56]. Icosahedral order has not been clearly linked to the dynamics of hard spheres, while the very notion of local order in more realistic glass-forming liquids (such binary mixtures of spheres, or larger molecules with internal degrees of freedom) is problematic and not easily defined. This makes the basis of the scenario very fragile, and its practical applicability for a particular material difficult.

## Aging and Off-equilibrium

### Why Aging?

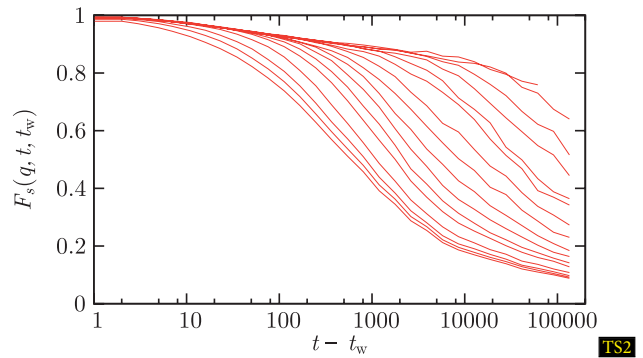
We have dedicated most of the above discussion to properties of materials approaching the glass transition at thermal equilibrium. We discussed a rich phenomenology and serious challenges for both our numerical and analytical capabilities to account for these phenomena. For most people, however, glasses are interesting below the glass transition, so deep in the glass phase that the material seems to be frozen forever in a seemingly arrested amorphous state, endowed with enough mechanical stability for a glass to retain, say, the liquid it contains (preferentially a nice red wine). Does this mean that there is no interesting physics in the glass state?

The answer is clearly ‘no’. There is still life (and physics) below the glass transition. We recall that for molecular glasses,  $T_g$  is defined as the temperature below which relaxation is too slow to occur within an experimen-

tal timescale. Much below  $T_g$ , therefore, the equilibrium relaxation timescale is so astronomically large that thermal equilibrium is out of reach. One enters therefore the realm of off-equilibrium dynamics. A full physical understanding of the non-equilibrium glassy state remains a central challenge [9,173].

A first consequence of studying materials in a time window smaller than equilibrium relaxation timescales is that the system can, in principle, remember its complete history, a most unwanted experimental situation since all details of the experimental protocol may then matter. The simplest protocol to study aging phenomena in the glass phase is quite brutal [152]: take a system equilibrated above the glass transition and suddenly quench it at a low temperature at a ‘waiting time’  $t_w = 0$  which corresponds to the beginning of the experiment. For  $t_w > 0$  the system is left unperturbed at constant temperature where it tries to slowly reach thermal equilibrium, even though it has no hope to ever get there. Aging means that the system never forgets the time  $t_w$  spent in the glass phase, its ‘age’. The evolution of one time quantities, e. g. the energy, as a function of time are not a good evidence of aging. In order to show that the system never equilibrates two time quantities, such as density-density or spin-spin correlation functions, are much more useful. A typical example is presented in Fig. 14 where the self-part of the intermediate function in Eq. (2) is shown for a Lennard-Jones molecular liquid at low temperature. Immediately after the quench, the system exhibits a relatively fast relaxation: particles still move substantially. However, when the age of the system increases, dynamics slows down and relaxation becomes much slower. When  $t_w$  becomes very large, relaxation becomes too slow to be followed in the considered time window and the system seems frozen on that particular timescale: it has become a glass. A striking feature conveyed by these data is that an aging system not only remains out-of-equilibrium for all practical purposes, but its typical relaxation time is in fact set by its age  $t_w$ . In simple cases, the effective relaxation time after waiting a time  $t_w$  scales at  $t_w$  itself, which means that since equilibration timescales have diverged,  $t_w$  is the only remaining relevant timescale in the problem.

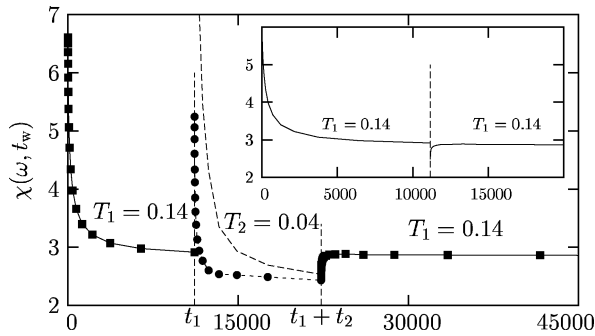
A popular interpretation of this phenomenon is given by considering trap models [40]. In this picture, reminiscent of the Goldstein view of the glass transition mentioned above [91], the system is described as a single particle evolving in a complex energy landscape with a broad distribution of trap depths—a paradigmatic mean-field approach. Aging in this perspective arises because the system visits traps that are increasingly deep when  $t_w$  increases, corresponding to more and more stable states. It



**Glasses and Aging: A Statistical Mechanics Perspective, Figure 14** Aging dynamics in a Lennard-Jones glass-forming liquid at low temperature. The system is quenched at time  $t_w=0$  at low  $T$ , where the temperature is kept constant. Two-time self-intermediate scattering functions are then measured for 20 logarithmically spaced waiting times  $t_w$  from  $t_w = 1$  to  $t_w = 10^5$  (from left to right). The relaxation becomes slower when  $t_w$  increases: the system ages

takes therefore more and more time for the system to escape, and the dynamics slows down with time, as observed in Fig. 14. This implies that any physical property of the glass becomes an age-dependent quantity in aging protocols, and more generally dependent on how the glass was prepared. One can easily imagine using this property to tune mechanical or optical characteristics of a material by simply changing the way it is prepared, like how fast it is cooled to the glassy state.

A real space alternative picture was promoted in particular in the context of spin glass studies, based on the ideas of scaling and renormalization [42,74]. The physical picture is that of a coarsening process, where the system develops long-range order by growing extended domains of lengthscale  $\ell(t_w)$ . On lengthscales less than  $\ell(t_w)$  the system has ordered since the quench at  $t_w = 0$ . The domain walls evolve in a random environment. In order to move they have to overcome free energy barriers. It is then assumed an activated dynamic scaling which states that the typical barrier to extend the domain from linear size  $\ell(t_w)$  to, say,  $2\ell(t_w)$  scales as  $\ell^\psi$ , where  $\psi$  is some ‘barrier’ exponent. Using the Arrhenius law to relate dynamics to barriers, one gets that aging corresponds to the logarithmic growth with time of spatially correlated domains,  $\ell \sim (T \log t_w)^{1/\psi}$ . A domain growth picture of aging in spin glasses can be directly confirmed by numerical simulations [113], only indirectly by experiments.



**Glasses and Aging: A Statistical Mechanics Perspective, Figure 15** Memory and rejuvenation effects obtained in the numerical simulation of a three-dimensional Heisenberg spin glass. There is a first aging step,  $0 < t_w < t_1$ , during which the system slowly tries to reach thermal equilibrium at temperature  $T_1$ . The system ‘rejuvenates’ in the second step at  $T_2$ ,  $t_1 < t < t_1 + t_2$ , and it restarts aging (rejuvenation). Finally in the third step, temperature is back to  $T_1$ , and memory of the first step is kept intact, as shown in the inset where relaxation during the second step of the experiment is taken away

#### Memory and Rejuvenation Effects

Since the complete history of a sample in the glass phase matters, there is no reason to restrain experimental protocols to the simple aging experiment mentioned above. Indeed, experimentalists have investigated scores of more elaborated protocols that have revealed an incredibly rich, and sometimes quite unexpected, physics [173]. We restrain ourselves here to a short discussion of memory and rejuvenation effects observed during temperature cycling experiments [148] (one can imagine applying a magnetic field or a mechanical constraint, be they constant in time or sinusoidal, etc.). These two effects were first observed in spin glasses, but the protocol was then repeated in many different materials, from polymers and organic liquids to disordered ferroelectrics. After several unsuccessful attempts, similar effects are now observed in numerical work as well. Results obtained from simulations of a three-dimensional Heisenberg spin glass [32] are presented in Fig. 15.

There are three steps in temperature cycling experiments [148]. The first one is a standard aging experiment, namely a sudden quench from high to low temperature at time  $t_w = 0$ . The system then ages for a duration  $t_1$  at constant temperature  $T_1$ . The system slowly relaxes towards equilibrium and its dynamics slows down, as observed in our spin glass example in Fig. 15 through the measurement of the magnetic susceptibility  $\chi(\omega, t_w)$ . Temperature is then suddenly shifted to  $T_2 < T_1$  at time  $t_1$ . There, the material restarts aging (almost) as if the first step had

not taken place. This is called ‘rejuvenation effect’, because the system seems to forget it is already ‘old’. At total time  $t_1 + t_2$ , temperature is then shifted back to its initial value  $T_1$ . Then, aging is found to proceed as a quasi-perfect continuation of the first step, as if the second step had not taken place. The system has kept the ‘memory’ of the first part of the experiment, despite the rejuvenation observed in the intermediate part. The memory effect becomes more spectacular when relaxation during the second step is removed, as in the inset of Fig. 15. The third relaxation appears indeed as a perfect continuation of the first one.

On top of being elegant and quite intriguing, such protocols are relevant because they probe more deeply the dynamics of aging materials, allowing one to ask more precise questions beyond the simplistic observation that ‘this material displays aging’. Moreover, the observation of similar effects in many different glassy materials implies that these effects are intrinsic to systems with slow dynamics. Interesting also are the subtle differences observed from one material to the other.

Several experimental, numerical and theoretical papers have been devoted to this type of experiments, and these effects are not ‘mysterious’ anymore [31]. A clear link between memory effects and typical lengthscales over which the slow dynamics takes place has been established. Because lengthscales depend so sensitively on timescales and on the working temperature, experiments performed at two different temperatures typically probe very different lengthscales, allowing the system to store memory of its state at different temperatures at different lengthscales [23,39]. In return, this link has been elegantly exploited to obtain a rather precise experimental estimate of dynamic lengthscales involved in the aging dynamics of spin glass materials [15], which seems to confirm the slow logarithmic growth law mentioned before.

Discussion of the rejuvenation effect is slightly more subtle. It is indeed not yet obvious that the effect as it is observed in computer simulations and reported, e.g., in Fig. 15 is exactly similar to the one observed in experiments. The difficulty comes from the fact that some seemingly innocuous details of the experimental protocol, such as the necessary use in experiments of finite cooling rates, in fact play a crucial role and influence the physics so that direct comparison between experiments and simulations is difficult. In numerical work, rejuvenation can be attributed to a gradual change with temperature of the nature of spatial correlations between spins that develop with time [23,32]. More drastic changes are predicted to occur in disordered systems as a result of the chaotic evolution with temperature of the metastable states in a spin glass (so-called ‘chaos effect’ [43]), that could also be respon-

1884 sible for the observed rejuvenation effect [107]. This sce-  
 1885 nario can be directly discarded in simulations, where spa-  
 1886 tial correlations can be easily measured and chaos sought  
 1887 (in vain) in a very direct manner. Understanding the very  
 1888 origin of the rejuvenation effect observed in experiments  
 1889 remains, however, a challenge.

1890 **Mean-Field Aging and Effective Temperatures**

1891 Theoretical studies of mean-field glassy models have pro-  
 1892 vided important insights into the aging dynamics of both  
 1893 structural and spin glasses [60,61]. Although such models  
 1894 are defined in terms of spin degrees of freedom interact-  
 1895 ing via infinite-ranged interactions, the deep connections  
 1896 between them and the mode-coupling theory of the glass  
 1897 transition make them serious candidates to investigate  
 1898 glassy states in general, not only thermodynamic proper-  
 1899 ties at thermal equilibrium but also non-equilibrium ag-  
 1900 ing dynamics. Despite their often reported ‘simplicity’,  
 1901 it took several years to derive a proper asymptotic so-  
 1902 lution of the long-time dynamics for a series of mean-  
 1903 field spin glasses [58]. These results have then triggered an  
 1904 enormous activity [57] encompassing theoretical, numeri-  
 1905 cal and also experimental work trying to understand fur-  
 1906 ther these results, and to check in more realistic systems  
 1907 whether they have some reasonable range of applicabil-  
 1908 ity beyond mean-field. This large activity, by itself, easily  
 1909 demonstrates the broad interest of these results.

1910 In these mean-field models, thermal equilibrium is  
 1911 never reached, and aging proceeds by downhill motion in  
 1912 an increasingly flat free energy landscape [119], with sub-  
 1913 tle differences between spin glass and structural glass mod-  
 1914 els. In both cases, however, time translational invariance  
 1915 is broken, and two-time correlation and response functions  
 1916 depend on both their time arguments. In fact, the exact  
 1917 dynamic solution of the equations of motion for time cor-  
 1918 relators displays behaviours in strikingly good agreement  
 1919 with the numerical results reported in Fig. 14.

1920 In these systems, the equations of motion in the aging  
 1921 regime involve not only time correlations, but also time-  
 1922 dependent response functions. At thermal equilibrium re-  
 1923 sponse and correlations are not independent, since the  
 1924 fluctuation-dissipation theorem (FDT) relates both quan-  
 1925 tities. In aging systems, there is no reason to expect the  
 1926 FDT to hold and both quantities carry, at least in princi-  
 1927 ple, distinct physical information. Again, the asymptotic  
 1928 solution obtained for mean-field models quantitatively es-  
 1929 tablishes that the FDT does not apply in the aging regime.  
 1930 Unexpectedly, the solution also shows that a generalized  
 1931 form of the FDT holds at large waiting times [60]. This  
 1932 is defined in terms of the two-time connected correlation

function for some generic observable  $A(t)$ , 1933

$$C(t, t_w) = \langle A(t)A(t_w) \rangle - \langle A(t) \rangle \langle A(t_w) \rangle, \quad (21) \quad 1934$$

with  $t \geq t_w$ , and the corresponding two-time (impulse) re- 1935  
 sponse function 1936

$$R(t, t_w) = T \left. \frac{\delta \langle A(t) \rangle}{\delta h(t_w)} \right|_{h=0}. \quad (22) \quad 1937$$

Here  $h$  denotes the thermodynamically conjugate field to 1938  
 the observable  $A$  so that the perturbation to the Hamilto- 1939  
 nian (or energy function) is  $\delta E = -hA$ , and angled brack- 1940  
 ets indicate an average over initial conditions and any 1941  
 stochasticity in the dynamics. Note that we have absorbed 1942  
 the temperature  $T$  in the definition of the response, for 1943  
 convenience. The associated generalized FDT reads then 1944

$$R(t, t_w) = X(t, t_w) \frac{\partial}{\partial t_w} C(t, t_w), \quad (23) \quad 1945$$

with  $X(t, t_w)$  the so-called fluctuation-dissipation ratio 1946  
 (FDR). At equilibrium, correlation and response func- 1947  
 tions are time translation invariant, depending only on 1948  
 $\tau = t - t_w$ , and equilibrium FDT imposes that  $X(t, t_w) = 1$  1949  
 at all times. A parametric fluctuation-dissipation (FD) plot 1950  
 of the step response or susceptibility 1951

$$\chi(t, t_w) = \int_{t_w}^t dt' R(t, t'), \quad 1952$$

against 1953

$$\Delta C(t, t_w) = C(t, t) - C(t, t_w), \quad 1954$$

is then a straight line with unit slope. These simplifications 1955  
 do not occur in non-equilibrium systems. But the defini- 1956  
 tion of an FDR through Eq. (23) becomes significant for 1957  
 aging systems [60,61]. In mean-field spin glass models the 1958  
 dependence of the FDR on both time arguments is only 1959  
 through the correlation function, 1960

$$X(t, t_w) \sim X(C(t, t_w)), \quad (24) \quad 1961$$

valid at large wait times,  $t_w \rightarrow \infty$ . For mean-field struc- 1962  
 tural glass models, the simplification (24) is even more spec- 1963  
 tacular since the FDR is shown to be characterized by 1964  
 only two numbers instead of a function, namely  $X \sim 1$  at 1965  
 short times (large value of the correlator) corresponding 1966  
 to a quasi-equilibrium regime, with a crossover to a non- 1967  
 trivial number,  $X \sim X^\infty$  for large times (small value of the 1968  
 correlator). This implies that parametric FD plots are sim- 1969  
 ply made of two straight lines with slope 1 and  $X^\infty$ , instead 1970



of the single straight line of slope 1 obtained at equilibrium.

Since any kind of behaviour is in principle allowed in non-equilibrium situations, getting such a simple, equilibrium-like structure for the FD relations is a remarkable result. This immediately led to the idea that aging systems might be characterized by an effective thermodynamic behaviour and the idea of quasi-equilibration at different timescales [59]. In particular, generalized FD relations suggest to define an effective temperature, as

$$T_{\text{eff}} = \frac{T}{X(t, t_w)}, \quad (25)$$

such that mean-field glasses are characterized by a unique effective temperature,  $T_{\text{eff}} = T/X^\infty$ . It is thought of as the temperature at which slow modes are quasi-equilibrated. One finds in general that  $0 < X^\infty < 1$ , such that  $T_{\text{eff}} > T$ , as if the system had kept some memory of its high temperature initial state.

The name ‘temperature’ for the quantity defined in Eq. (25) is not simply the result of a dimensional analysis but has a deeper, physically appealing meaning that is revealed by asking the following questions. How does one measure temperatures in a many-body system whose relaxation involves well-separated timescales? What is a thermometer (and a temperature) in a far from equilibrium aging material? Answers are provided in Refs. [59, 120] both for mean-field models and for additional toy models with multiple relaxation timescales. The idea is to couple an additional degree of freedom, such as a harmonic oscillator,  $x(t)$ , which plays the role of the thermometer operating at frequency  $\omega$ , to an observable of interest  $A(t)$  via a linear coupling,  $-\lambda x(t)A(t)$ . Simple calculations show then that the thermometer ‘reads’ the following temperature,

$$\frac{1}{2}K_B T_{\text{meas}}^2 \equiv \frac{1}{2}\omega^2 \langle x^2 \rangle = \frac{\omega C'(\omega, t_w)}{2\chi''(\omega, t_w)}, \quad (26)$$

where  $C'(\omega, t_w)$  is the real part of the Fourier transform of Eq. (21), and  $\chi(\omega, t_w)$  the imaginary part of the Fourier transform of Eq. (22), with  $h = \lambda x$ . The relation (26) indicates that the bath temperature is measured,  $T_{\text{meas}} = T$ , if frequency is high and FDT is satisfied, while  $T_{\text{meas}} = T_{\text{eff}} > T$  if frequency is slow enough to be tuned to that of the slow relaxation in the aging material. The link between the FDR in Eq. (23) and the effective temperature measured in Eq. (26) was numerically confirmed in the computer simulation of a glassy molecular liquid in Ref. [19].

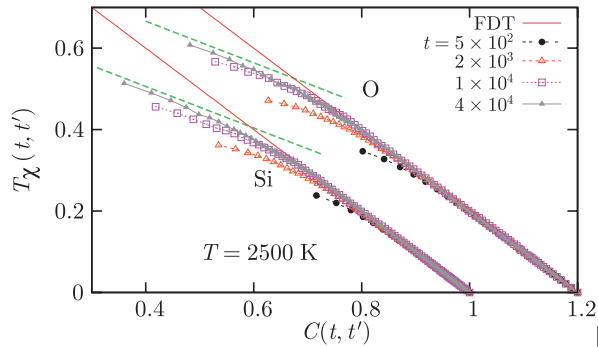
More generally, relaxation in glassy systems occurs in well-separated time sectors [61]; it is then easy to imagine

that each sector could be associated with an effective temperature [120]. A thermodynamic interpretation of effective temperatures has also been put forward, relating them to the concept of replica symmetry breaking [78]. Interestingly, the full-step or one-step replica symmetry breaking schemes needed to solve the static problem in these models have a counterpart as the FDR being a function or a number, respectively, in the aging regime. Moreover, we note that these modern concepts are related to, but make much more precise, older ideas of quasi-equilibrium and fictive temperatures in aging glasses [152].

Taken together, these results make the mean-field description of aging very appealing, and they nicely complement the mode-coupling/RFOT description of the equilibrium glass transition described above. Moreover, they have set the agenda for a large body of numerical and experimental work, as reviewed in [57]. In Fig. 16 we present recent numerical data obtained in an aging silica glass [30], presented in the form of a parametric response-correlation plot. The measured correlation functions are the self-part of the intermediate scattering functions defined in Eq. (2), while the conjugated response functions quantify the response of particle displacements to a spatially modulated field conjugated to the density. Plots for silicon and oxygen atoms at different ages of the system are presented. They seem to smoothly converge towards a two-straight line plot, as obtained in mean-field models (note, however, that this could be just a pre-asymptotic, finite “ $t_w$ ”, effect). Moreover, the second, non-trivial part of the plot is characterized by a slope that appears to be independent of the species, and of the wavevector chosen to quantify the dynamics, in agreement with the idea of a unique asymptotic value of the FDR, possibly related to a well-defined effective temperature.

### Beyond Mean-Field

Despite successes such as shown in Fig. 16, the broader applicability of the mean-field scenario of aging dynamics remains unclear, however. While some experiments and simulations indeed seem to support the existence of well-behaved effective temperatures [1,92,164], other studies also reveal the limits of the mean-field scenario. Experiments have for instance reported anomalously large FDT violations associated with intermittent dynamics [11,12,44,45], while theoretical studies of model systems have also found non-monotonic or even negative response functions [68,118,140,162], and ill-defined or observable-dependent FDRs [73]. In principle, these discrepancies with mean-field predictions are to be expected, since there are many systems of physical interest



**Glasses and Aging: A Statistical Mechanics Perspective, Figure 16** Parametric correlation-response plots measured in the aging regime of a numerical model for a silica glass, SiO<sub>2</sub> [30]. The plots for both species smoothly converges towards a two-straight line plot of slope 1 at short times (large C values), and of slope  $X^\infty \approx 0.51$  at large times (small values of C), yielding an effective temperature of about  $T_{\text{eff}} = T/X^\infty \approx 4900$  K. Note that the glass transition temperature of SiO<sub>2</sub> is 1446 K

coarsening systems in  $d \geq 2$ , one has  $X^\infty = 0$ , or equivalently an infinite effective temperature,  $T_{\text{eff}} = \infty$ . The case  $d = 1$  is special because  $T_c = 0$  and the response function remains dominated by the domain walls, which yields the non-trivial value  $X^\infty = 1/2$  [89].

Another special case has retained attention. When the quench is performed at  $T = T_c$ , there is no more distinction between walls and domains and the above argument yielding  $X^\infty = 0$  does not hold. Instead one studies the growth with time of critical fluctuations, with  $\xi(t_w) \sim t_w^{1/z}$  the correlation length at time  $t_w$ , where  $z$  is the dynamic exponent. Both correlation and response functions become non-trivial at the critical point [90]. It proves useful in that case to consider the dynamics of the Fourier components of the magnetization fluctuations,  $C_q(t, t_w) = \langle m_q(t)m_{-q}(t_w) \rangle$ , and the conjugated response  $R_q(t, t_w) = \langle \delta \langle m_q(t) \rangle \delta h_{-q}(t_w) \rangle$ . From Eq. (23) a wavevector dependent FDR follows,  $X_q(t, t_w)$ , which has interesting properties [128] (see [47] for a review).

In dimension  $d = 1$ , it is possible to compute  $X_q(t, t_w)$  exactly in the aging regime at  $T = T_c = 0$ . An interesting scaling form is found, and numerical simulations performed for  $d > 1$  confirm its validity:

$$X_q(t, t_w) = \mathcal{X}(q^2 t_w), \quad (27)$$

where the scaling function  $\mathcal{X}(x)$  is  $\mathcal{X}(x \rightarrow \infty) \rightarrow 1$  at small lengthscale,  $q\xi \gg 1$ , and  $\mathcal{X}(x \rightarrow 0) \rightarrow 1/2$  (in  $d = 1$ ) at large distance,  $q\xi \ll 1$ ; recall that for  $z = 2$  in that case.

Contrary to mean-field systems where geometry played no role, here the presence of a growing correlation lengthscale plays a crucial role in the off-equilibrium regime since  $\xi(t_w)$  allows one to discriminate between fluctuations that satisfy the FDT at small lengthscale,  $X_q \sim 1$ , and those at large lengthscale which are still far from equilibrium,  $0 < X_q \sim X^\infty < 1$ . These studies suggest therefore that generalized fluctuation-dissipation relation in fact have a strong lengthscale dependence—a result which is not predicted by mean-field approaches.

Another interesting result is that the FDT violation for global observables (i. e. those at  $q = 0$ ) takes a particularly simple form, since the introduction of a single number is sufficient, the FDR at zero wavevector,  $X_{q=0}(t, t_w) \equiv X^\infty = 1/2$  (in  $d = 1$ ). This universal quantity takes non-trivial values in higher dimension, e. g.  $X^\infty \approx 0.34$  is measured in  $d = 2$  [128]. This shows that the study of global rather than local quantities makes the measurement of  $X^\infty$  much easier. Finally, having a non-trivial value of  $X^\infty$  for global observables suggests that the possibility to define an effective temperature remains

in which the dynamics are not of mean-field type, displaying both activated processes and spatial heterogeneity.

It is thus an important task to understand from the theoretical point of view when the mean-field concept of an FDR-related effective temperature remains viable. However, studying theoretically the interplay between relevant dynamic lengthscales and thermally activated dynamics in the non-equilibrium regime of disordered materials is clearly a challenging task. Nevertheless, this problem has been approached in different ways, as we briefly summarize in this subsection.

A first class of system that displays aging and spatial heterogeneity is given by coarsening systems. The paradigmatic situation is that of an Ising ferromagnetic model (with a transition at  $T_c$ ) suddenly quenched in the ferromagnetic phase at time  $t_w = 0$ . For  $t_w > 0$  domains of positive and negative magnetizations appear and slowly coarsen with time. The appearance of domains that grow with time proves the presence of both aging and heterogeneity in this situation.

The case where the quench is performed down to  $T < T_c$  is well understood. The system becomes scale invariant [41], since the only relevant lengthscale is the growing domain size,  $\ell(t_w)$ . Correlation functions display aging, and scale invariance implies that  $C(t, t_w) \sim f(\ell(t)/\ell(t_w))$ . Response functions can be decomposed into two contributions [8,17]: one part stems from the bulk of the domains and behaves as the equilibrium response, and a second one from the domain walls and becomes vanishingly small in the long time limit where  $\ell(t_w) \rightarrow \infty$  and the density of domain walls vanishes. This implies that for

valid, but it has become a more complicated object, related to global fluctuations on large lengthscale.

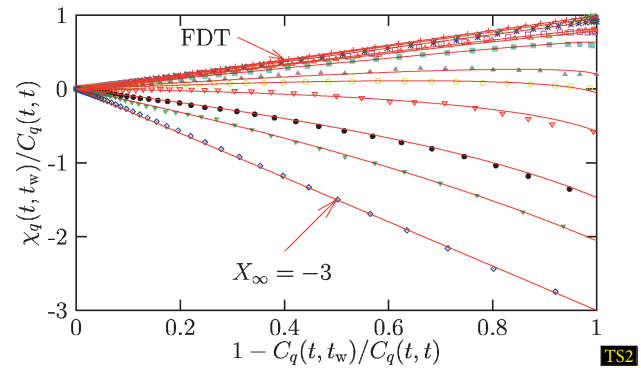
Kinetically constrained spin models represent a second class of non-mean-field systems whose off-equilibrium has been thoroughly studied recently [125]. This is quite a natural thing to do since these systems have local, finite ranged interactions, and they combine the interesting features of being defined in terms of (effective) microscopic degrees of freedom, having local dynamical rules, and displaying thermally activated and heterogeneous dynamics.

The case of the Fredrickson–Andersen model, described in Sect. “Some Theory and Models”, has been studied in great detail [125], and we summarize the main results. Here, the relevant dynamic variables are the Fourier components of the mobility field, which also correspond in that case to the fluctuations of the energy density. Surprisingly, the structure of the generalized fluctuation-dissipation relation remains once more very simple. In particular, in dimension  $d > 2$ , one finds a scaling form similar to (27),  $X_q(t, t_w) = X(q^2 t_w)$ , with a well-defined limit at large distance  $X_{q=0}(t, t_w) \equiv X^\infty$ . The deep analogy with critical Ising models stems from the fact that mobility defects in KCMs diffuse in a way similar to domain walls in coarsening Ising models. It is in fact by exploiting this analogy that analytic results are obtained in the aging regime of the Fredrickson–Andersen model [130].

There is however a major qualitative difference between the two families of model. The (big!) surprise lies in the sign of the asymptotic FDR, since calculations show that [129]

$$X^\infty = -3, \quad d > 2.$$

In dimension  $d = 1$ , one finds  $X_{q=0}(t, t_w) = f(t/t_w)$  with  $X_{q=0}(t \rightarrow \infty, t_w) = (3\pi)(16 - 6\pi) \approx -3.307$ . Numerical simulations confirm these calculations. In Fig. 17, we show such a comparison between simulations (symbols) and theory (lines) in the case of the  $d = 3$  Fredrickson–Andersen model [129]. Fourier components of the mobility field yield parametric FD plots that follow scaling with the variable  $q^2 t_w$ , as a direct result of the presence of a growing lengthscale for dynamic heterogeneity,  $\xi(t_w) \sim \sqrt{t_w}$ . Again, generalized fluctuation-dissipation relations explicitly depend on the spatial lengthscale considered, unlike in mean-field studies. In Fig. 17, the limit  $q = 0$  corresponding to global observables is also very interesting since the plot is a pure straight line, as in equilibrium. Unlike equilibrium, however, the slope is not 1 but -3. A negative slope in this plot means a negative FDR, and therefore suggests a negative effective temperature, an very non-intuitive result at first sight.



**Glasses and Aging: A Statistical Mechanics Perspective, Figure 17** Parametric response-correlation plots for the Fourier components of the mobility field in the  $d = 3$  Fredrickson–Andersen model. Symbols are from simulations, lines from analytic calculations, and wavevectors decrease from top to bottom. The FDT is close to being satisfied at large  $q$  corresponding to local equilibrium. At larger distance deviations from the FDT are seen, with an asymptotic FDR which becomes negative. Finally, for energy fluctuations at  $q = 0$  (bottom curve), the plot becomes a pure straight line of (negative!) slope  $-3$ , as a result of thermally activated dynamics

Negative response functions in fact directly follows from the thermally activated nature of the dynamics of these models [129]. First, one should note that the global observable shown in Fig. 17 corresponds to fluctuations of the energy,  $e(t_w)$ , whose conjugated field is temperature. In the aging regime the system slowly drifts towards equilibrium. Microscopic moves result from thermally activated processes, corresponding to the local crossing of energy barriers. An infinitesimal change in temperature,  $T \rightarrow T + \delta T$  with  $\delta T > 0$ , accelerates these barrier crossings and makes the relaxation dynamics faster. The energy response to a positive temperature pulse is therefore negative,  $\delta e < 0$ , which directly yields  $\delta e/\delta T < 0$ , which explains the negative sign of the FDR. This result does not hold in mean-field glasses, where thermal activation plays no role.

Finally, another scenario holds for local observables in some KCMs when kinetic constraints are stronger, such as the East model [125] or a bidimensional triangular plaquette model [100]. Here, relaxation is governed by a hierarchy of energy barriers that endow the systems with specific dynamic properties. In the aging regime following a quench, in particular, the hierarchy yields an energy relaxation that arises in discrete steps which take place on very different timescales, reminiscent of the ‘time sectors’ encountered in mean-field spin glasses. Surprisingly, it is found that to each of these discrete relaxations one can associate a well-defined (positive) value of the fluctuation-

2224 dissipation ratio, again reminiscent of the dynamics of  
2225 mean-field spin glass models. Therefore, even in mod-  
2226 els that are very far from the mean-field limit the phys-  
2227 ical picture of a slow relaxation taking place on multiple  
2228 timescales with each timescale characterized by an effec-  
2229 tive temperature seems to have some validity.

### 2230 Driven Glassy Materials

2231 We have introduced aging phenomena with the argument  
2232 that in a glass phase, the timescale to equilibrate becomes  
2233 so long that the system always remembers its complete his-  
2234 tory. This is true in general, but one can wonder whether it  
2235 is possible to invent a protocol where the material history  
2236 could be erased, and the system ‘rejuvenated’ [132]. This  
2237 concept has been known for decades in the field of poly-  
2238 mer glasses, where complex thermo-mechanical histories  
2239 are often used.

2240 Let us consider an aging protocol where the system  
2241 is quenched to low temperature at time  $t_w = 0$ , but the  
2242 system is simultaneously forced by an external mechan-  
2243 ical constraint. Experimentally one finds that a station-  
2244 ary state can be reached, which explicitly depends on the  
2245 strength of the forcing: a system which is forced more  
2246 strongly relaxes faster than a less solicited material, a phe-  
2247 nomenon called ‘shear-thinning’. The material has there-  
2248 fore entered a driven steady state, where memory of its age  
2249 is no longer present and dynamics has become stationary:  
2250 aging is stopped.

2251 Many studies of these driven glassy states have been  
2252 performed in recent years. In the language of the jamming  
2253 phase diagram in Fig. 4, these correspond to studies of the  
2254 (Temperature, Load) plane for molecular liquids, or the  
2255 (1/Density, Load) plane for colloidal systems. The former  
2256 studies are relevant for the rheology of supercooled liquids  
2257 and glasses, and the  $T \ll T_g$  limit corresponds to studies  
2258 of the plasticity of amorphous solids, a broad field in it-  
2259 self. In the colloidal world, such studies are also relevant  
2260 for the newly-defined field of the rheology of ‘soft glassy  
2261 materials’. These materials are (somewhat tautologically)  
2262 defined as those for which the non-linear rheological be-  
2263 haviour is believed to result precisely from the competi-  
2264 tion between intrinsically slow relaxation processes and  
2265 an external forcing [150]. It is believed that the rheology  
2266 of dense colloidal suspensions, foams, emulsions, binary  
2267 mixtures, or even biophysical systems are ruled by such  
2268 a competition, quite a broad field of application indeed.

2269 From the point of view of statmech modeling, soft  
2270 glassy rheology can be naturally studied from the very  
2271 same angles as the glass transition itself. As such trap mod-  
2272 els [150,151], mean-field spin glasses [18] and the related

mode-coupling theory approach [83,134] have been ex-  
2273 plicitly extended to include an external mechanical forc-  
2274 ing. In all these cases, one finds that a driven steady state  
2275 can be reached and aging is indeed expected to stop at  
2276 a level that depends on the strength of the forcing. Many  
2277 of the results obtained in aging systems about the proper-  
2278 ties of an effective temperature are also shown to apply in  
2279 the driven case, as shown both theoretically [18] and nu-  
2280 merically [16]. A most interesting aspect is that the broad  
2281 relaxation spectra predicted to occur in glassy materials  
2282 close to a glass transition directly translate into ‘anoma-  
2283 lous’ laws both for the linear rheological behaviour (seen  
2284 experimentally in the broad spectrum of elastic,  $G'(\omega)$ ,  
2285 and loss,  $G''(\omega)$ , moduli), and the non-linear rheological  
2286 behaviour (a strong dependence of the viscosity  $\eta$  upon  
2287 the shear rate  $\dot{\gamma}$ ).  
2288

### 2289 Future Directions

The problem of the glass transition, already very exciting  
2290 in itself, has ramifications well beyond the physics of su-  
2291 percooled liquids. Glassy systems figures among the even  
2292 larger class of ‘complex systems’. These are formed by a set  
2293 of interacting degrees of freedom that show an emergent  
2294 behaviour: as a whole they exhibit properties not obvious  
2295 from the properties of the individual parts. As a conse-  
2296 quence the study of glass-formers as statistical mechanics  
2297 model characterized by frustrated interactions is a fertile  
2298 ground to develop new concepts and techniques that will  
2299 likely be applied to other physical, and more generally, sci-  
2300 entific situations.  
2301

2302 An example, already cited in this review, are the recent  
2303 progress obtained in computer science and information  
2304 theory [55] using techniques originally developed for spin  
2305 glasses and structural glasses. More progress is certainly  
2306 expected in the future along these interdisciplinary routes.  
2307 Concerning physics, glassiness is such an ubiquitous and,  
2308 yet as we showed, rather poorly understood problem that  
2309 many developments are very likely to take place in the next  
2310 decade.

2311 Instead of guessing future developments of the field  
2312 (and then very likely be proven wrong) we prefer to list  
2313 a few problems we would like to see solved in the next  
2314 years.

- 2315 • Are the jamming transitions of granular media and col-  
2316 loids related to the glass transition of supercooled liq-  
2317 uids? If yes, what is the common physical mechanism  
2318 behind the dramatic slowing down?
- 2319 • Is the glass transition related to a true phase transition?  
2320 If yes, a static or a dynamic one? A finite or zero tem-  
2321 perature one?

- 2322 • Do RFOT, defects models, or frustration-based theory  
2323 form the correct starting points of ‘the’ theory of the  
2324 glass transition?
- 2325 • Is MCT really a useful theory for the first decades of  
2326 slowing down of the dynamics? Can one find direct ev-  
2327 idence that an avoided MCT transition exists and con-  
2328 trols the dynamics?
- 2329 • What is the correct physical picture for the low temper-  
2330 ature phase of glass-forming liquids and spin glasses?
- 2331 • Are there general principles governing off-equilibrium  
2332 equilibrium dynamics, and in particular aging and  
2333 sheared materials?
- 2334 • Do non-disordered, finite-dimensional, finite-range  
2335 statmech model exist that display a thermodynamically  
2336 stable amorphous phase at low temperature?

2337 Finally, notice that we did not discuss possible inter-  
2338 plays between glassiness and quantum fluctuations. This  
2339 is a very fascinating topic. Quantum glassiness, and more  
2340 generally, slow quantum dynamics are research subjects  
2341 which are still in their infancies but that will likely undergo  
2342 exciting developments in the near future.

### 2343 Acknowledgements

2344 We thank C. Marchetti for inviting us to write this review  
2345 and the collaborators who worked with us on glass physics.  
2346 We thank J.-P. Bouchaud, A. Lefèvre, T. Sarlat for a care-  
2347 ful reading of our manuscript and suggestions. Our work  
2348 is supported by ANR Grants CHEF, TSANET and DYN-  
2349 HET.

### 2350 Bibliography

#### 2351 Primary Literature

- 2352 1. Abou B, Gallet F (2004) **TS3** Phys Rev Lett 93:160603
- 2353 2. Adam G, Gibbs JH (1958) J Chem Phys 43:139
- 2354 3. Adhikari AN, Capurso NA, Bingemann D (2007) J Chem Phys  
2355 127:114508
- 2356 4. Allen M, Tildesley D (1987) Computer Simulation of Liquids.  
2357 Oxford University Press, Oxford
- 2358 5. Angell CA (1997) J Res NIST 102:171
- 2359 6. Angell CA (1995) Science 267:1924
- 2360 7. Appignanesi GA, Rodriguez JA Fris, Montani RA, Kob W (2006)  
2361 Phys Rev Lett 96:057801
- 2362 8. Barrat A (1998) Phys Rev E 57:3629
- 2363 9. Barrat J-L, Dalibard J, Feigelman M, Kurchan J (eds) (2003)  
2364 Slow relaxations and nonequilibrium dynamics in condensed  
2365 matter. Springer, Berlin
- 2366 10. Bassler H (1987) Phys Rev Lett 58:767
- 2367 11. Bellon L, Ciliberto S, Laroche C (2001) Europhys Lett 53:511
- 2368 12. Bellon L, Ciliberto S (2002) Physica D 168:325
- 2369 13. Bengtzelius U, Götze W, Sjölander A (1984) J Phys C 17:5915
- 2370 14. Bennemann C, Donati C, Baschnagel J, Glotzer SC (1999) Na-  
2371 ture 399:246;

- Lacevic N, Starr FW, Schroder TB, Glotzer SC (2003) J Chem  
2372 Phys 119:7372 **TS4** 2373
15. Bert F, Dupuis V, Vincent E, Hammann J, Bouchaud J-P (2004)  
2374 Phys Rev Lett 92:167203 2375
16. Berthier L, Barrat J-L (2002) J Chem Phys 116:6228 2376
17. Berthier L, Barrat J-L, Kurchan J (1999) Eur Phys J B 11:635 2377
18. Berthier L, Barrat J-L, Kurchan J (2000) Phys Rev E 61:5464 2378
19. Berthier L, Barrat J-L (2002) Phys Rev Lett 89:095702 2379
20. Berthier L, Biroli G, Bouchaud J-P, Cipelletti L, D El Masri,  
2380 L'Hôte D, Ladieu F, Pierno M (2005) Science 310:1797 2381
21. Berthier L, Biroli G, Bouchaud J-P, Kob W, Miyazaki K, Reich-  
2382 man DR (2007) J Chem Phys 126:184503 2383
22. Berthier L, Biroli G, Bouchaud J-P, Kob W, Miyazaki K, Reich-  
2384 man DR (2007) J Chem Phys 126:184504 2385
23. Berthier L, Bouchaud J-P (2002) Phys Rev B 66:054404 2386
24. Berthier L, Chandler D, Garrahan JP (2005) Europhys Lett  
2387 69:320 2388
25. Berthier L, Garrahan JP (2003) J Chem Phys 119:4367 2389
26. Berthier L, Garrahan JP (2005) J Phys Chem B 109:3578 2390
27. Berthier L, Kob W (2007) J Phys: Condens Matter 19:205130 2391
28. Berthier L (2004) Phys Rev E 69:020201(R) 2392
29. Berthier L (2007) Phys Rev E 76:011507 2393
30. Berthier L (2007) Phys Rev Lett 98:220601 2394
31. Berthier L, Viasnoff V, White O, Orlyanchik V, Krzakala F, in Ref-  
2395 erence [9] 2396
32. Berthier L, Young AP (2005) Phys Rev B 71:214429 2397
33. Binder K, Kob W (2005) Glassy materials and disordered solids.  
2398 World Scientific, Singapore 2399
34. Biroli G, Bouchaud J-P, Miyazaki K, Reichman DR (2006) Phys  
2400 Rev Lett 97:195701 2401
35. Biroli G, Bouchaud J-P, Tarjus G (2005) J Chem Phys  
2402 123:044510 2403
36. Biroli G, Bouchaud JP (2004) Europhys Lett 67:21 2404
37. Biroli G, Mézard M (2001) Phys Rev Lett 88:025501 2405
38. Bouchaud J-P, Biroli G (2004) J Chem Phys 121:7347 2406
39. Bouchaud J-P, Dupuis V, Hammann J, Vincent E (2001) Phys  
2407 Rev B 65:024439 2408
40. Bouchaud JP (1992) J Phys I France 2:1705 2409
41. Bray AJ (1994) Adv Phys 43:357 2410
42. Bray AJ, Moore MA (1984) J Phys C 17:L463; and in (1987)  
2411 Heidelberg Colloquim on Glassy Dynamics In: van Hemmen  
2412 JL, Morgenstern I (eds), Lectures Notes in Physics, vol 275. 2413  
Springer, Berlin 2414
43. Bray AJ, Moore MA (1987) Phys Rev Lett 58:57 2415
44. Buisson L, Bellon L, Ciliberto S (2003) J Phys Condens Matter  
2416 15:S1163 2417
45. Buisson L, Ciliberto S, Garcimartin A (2003) Europhys Lett  
2418 63:603 2419
46. Butler S, Harrowell P (1991) J Chem Phys 95:4454 ((1991) J  
2420 Chem Phys 95:4466) 2421
47. Calabrese P, Gambassi A (2005) J Phys A 38:R133 2422
48. Castellani T, Cavagna A (2005) J Stat Mech P05012 2423
49. Cavagna A, Grigera TS, Verrocchio P (2007) Phys Rev Lett  
2424 98:187801 2425
50. Chandler D, Garrahan JP, Jack RL, Maibaum L, Pan AC (2006)  
2426 Phys Rev E 74:051501 2427
51. Chaudhuri P, Berthier L, Kob W (2007) Phys Rev Lett  
2428 99:060604 2429
52. Cheng Z, J, Chaikin PM, Phan S, Russel WB (2002) Phys Rev E  
2430 65:041405 2431
53. Cohen MH, Grest GS (1982) Phys Rev B 26:6313 2432

**TS3** Please provide for all articles a title if possible.

**TS4** Is this a new reference?

- 2433 54. Coluzzi B, Verrocchio P (2002) *J Chem Phys* 116:3789
- 2434 55. Mézard M, Bouchaud J-P, Dalibard J (eds) (2007) *Complex systems*. Springer, Berlin
- 2435 56. Coslovich D, Pastore G (2007) *J Chem Phys* 127:124504
- 2436 57. Crisanti A, Ritort F (2003) *J Phys A* 36:R181
- 2437 58. Cugliandolo LF in Reference [9]
- 2438 59. Cugliandolo LF, Kurchan J, Peliti L (1997) *Phys Rev E* 55:3898
- 2439 60. Cugliandolo LF, Kurchan J (1993) *Phys Rev Lett* 71:173
- 2440 61. Cugliandolo LF, Kurchan J (1994) *J Phys A* 27:5749
- 2441 62. D'Anna G, Gremaud G (2001) *Nature* 413:407
- 2442 63. Dalle-Ferrier C, Thibierge C, Alba-Simionesco C, Berthier L, Biroli G, Bouchaud J-P, Ladieu F, L'Hôte D, Tarjus G (2007) *Phys Rev E* 76:041510
- 2443 64. Das SP, Mazenko GF (1986) *Phys Rev A* 34:2265
- 2444 65. Dauchot O, Marty G, Biroli G (2005) *Phys Rev Lett* 95:265701
- 2445 66. Debenedetti PG (1996) *Metastable liquids*. Princeton University Press, Princeton
- 2446 67. Debenedetti PG, Stillinger FH (2001) *Nature* 410:259
- 2447 68. Depken M, Stinchcombe R (2005) *Phys Rev E* 71:065102
- 2448 69. Donati C, Douglas J, Kob W, Plimpton SJ, Poole PH, Glotzer SC (1998) *Phys Rev Lett* 80:2338
- 2449 70. Downton MT, Kennett MP (2007) *Phys Rev E* 76:031502
- 2450 71. Dzero M, Schmalian J, Wolynes PG (2005) *Phys Rev B* 72:100201
- 2451 72. Ediger MD (2000) *Annu Rev Phys Chem* 51:99
- 2452 73. Fielding S, Sollich P (2002) *Phys Rev Lett* 88:050603
- 2453 74. Fisher DS, Huse DA (1986) *Phys Rev Lett* 56:1601
- 2454 75. Franck FC (1952) *Proc R Soc London* 215:43
- 2455 76. Franz S, Donati C, Parisi G, Glotzer SC (1999) *Philos Mag B* 79:1827
- 2456 77. Franz S, Mulet R, Parisi G (2002) *Phys Rev E* 65:021506
- 2457 78. Franz S, Mézard M, Parisi G, Peliti L (1998) *Phys Rev Lett* 81:1758
- 2458 79. Franz S, Parisi G (2000) *J Phys Condens Matter* 12:6335
- 2459 80. Franz S, Stat J (2005) *Mech P04001* (2006) *Europhys Lett* 73:492
- 2460 81. Fredrickson GH, Andersen HC (1984) *Phys Rev Lett* 53:1244
- 2461 82. Fredrickson GH, Brawer SA (1986) *J Chem Phys* 84:3351
- 2462 83. Fuchs M, Cates ME (2002) *Phys Rev Lett* 89:248304
- 2463 84. Garrahan JP, Chandler D (2002) *Phys Rev Lett* 89:035704
- 2464 85. Garrahan JP, Chandler D (2003) *Proc Natl Acad Sc USA* 100:9710
- 2465 86. Garrahan JP (2002) *J Phys Condens Matter* 14:1571
- 2466 87. Glarum SH (1960) *J Chem Phys* 33:639
- 2467 88. Gleim T, Kob W, Binder K (1998) *Phys Rev Lett* 81:4404
- 2468 89. Godrèche C, Luck J-M (2000) *J Phys A* 33:1151; Lippiello E, Zannetti M (2000) *Phys Rev E* 61:3369
- 2469 90. Godrèche C, Luck J-M (2000) *J Phys A* 33:9141
- 2470 91. Goldstein M (1969) *J Chem Phys* 51:3728
- 2471 92. Grigera TS, Israeloff NE (1999) *Phys Rev Lett* 83:5038
- 2472 93. Gross J, Mézard M (1984) *Nucl Phys B* 240:431
- 2473 94. Götze W (1999) *J Phys Condens Matter* 11:A1
- 2474 95. Hansen JP, McDonald IR (1986) *Theory of Simple Liquids*. Academic, London
- 2475 96. Hodge I (1997) *J Res NIST* 102:195
- 2476 97. Holyst R (2001) *Physica A* 292:255
- 2477 98. Horbach J, Kob W (2001) *Phys Rev E* 64:041503
- 2478 99. Hurley MM, Harrowell P (1995) *Phys Rev E* 52:1694
- 2479 100. Jack RL, Berthier L, Garrahan JP (2006) *J Stat Mech* P12005
- 2480 101. Jack RL, Berthier L, Garrahan JP (2005) *Phys Rev E* 72:016103
- 2481 102. Jack RL, Garrahan JP (2005) *J Chem Phys* 123:164508
- 2482 103. Jack RL, Mayer P, Sollich P (2006) *J Stat Mech Theory Exp* P03006
- 2483 104. Jaeger HM, Nagel SR, Behringer RP (1996) *Rev Mod Phys* 68:1259
- 2484 105. Johari GP (2000) *J Chem Phys* 112:8958
- 2485 106. Jung Y, Garrahan JP, Chandler D (2004) *Phys Rev E* 69:061205
- 2486 107. Jönsson PE, Mathieu R, Nordblad P, Yoshino H, H Aruga Katori, Ito A (2004) *Phys Rev B* 70:174402
- 2487 108. Kauzmann AW (1948) *Chem Rev* 43:219
- 2488 109. Kegel WK, van Blaaderen A (2000) *Science* 287:290
- 2489 110. Keys AS, Abate AR, Glotzer SC, Durian DJ (2007) *Nat Phys* 3:260
- 2490 111. Kirkpatrick TR, Thirumalai D (1987) *Phys Rev Lett* 58:2091 (Kirkpatrick TR, Wolynes PG (1987) *Phys Rev A* 35:3072) **TS4**
- 2491 112. Kirkpatrick TR, Thirumalai D, Wolynes PG (1989) *Phys Rev A* 40:1045
- 2492 113. Kisker J, Santen L, Schreckenberg M, Rieger H (1996) *Phys Rev B* 53:6418
- 2493 114. Kivelson D, Kivelson SA, Zhao X-L, Nussinov Z, Tarjus G (1995) *Physica A* 219:27
- 2494 115. Kob W, Andersen HC (1993) *Phys Rev E* 48:4364
- 2495 116. Kob W, Donati C, Plimpton SJ, Poole PH, Glotzer SC (1997) *Phys Rev Lett* 79:2827
- 2496 117. Krzakala F, Montanari A, Ricci-Tersenghi, Semerjian G, Zdeborová L (2007) 104:10318
- 2497 118. Krzakala F (2005) *Phys Rev Lett* 94:077204
- 2498 119. Kurchan J, Laloux L (1996) *J Phys A* 29:1929
- 2499 120. Kurchan J (2005) *Nature* 433:222
- 2500 121. Larson RG (1999) *The Structure and Rheology of Complex Fluids*. Oxford University Press, New York
- 2501 122. Leutheusser E (1984) *Phys Rev A* 29:2765
- 2502 123. Lipowski A, Johnston D, Espriu D (2000) *Phys Rev E* 62:3404
- 2503 124. Liu AJ, Nagel SR (1998) *Nature* 396:21
- 2504 125. Léonard S, Mayer P, Sollich P, Berthier L, Garrahan JP (2007) *J Stat Mech* P07017
- 2505 126. Mapes MK, Swallen SF, Ediger MD (2006) *J Chem Phys* 124:054710
- 2506 127. Marty G, Dauchot O (2005) *Phys Rev Lett* 94:015701
- 2507 128. Mayer P, Berthier L, Garrahan JP, Sollich P (2003) *Phys Rev E* 68:016116
- 2508 129. Mayer P, Léonard S, Berthier L, Garrahan JP, Sollich P (2006) *Phys Rev Lett* 96:030602
- 2509 130. Mayer P, Sollich P (2007) *J Phys A* 40:5823
- 2510 131. McCullagh GD, Cellai D, Lawlor A, Dawson KA, *Phys. Rev. E* 71:030102 (2005)
- 2511 132. McKenna GB, Kovacs AJ (1984) *Polym Eng Sci* 24:1131
- 2512 133. Menon N, Nagel SR, *Phys. Rev. Lett* 74:1230 (1995); Fernandez LA, Martin V-Mayor, Verrocchio P (2006) *Phys Rev E* 73:020501; and [49]
- 2513 134. Miyazaki K, Reichman DR (2002) *Phys Rev E* 66:050501(R)
- 2514 135. Monasson R (1995) *Phys Rev Lett* 75:2847
- 2515 136. Mézard M, Parisi G (1999) *Phys Rev Lett* 82:747
- 2516 137. Mézard M, Parisi G, Virasoro M (1988) *Spin Glass Theory and Beyond*. World Scientific, Singapore
- 2517 138. Nauroth M, Kob W (1997) *Phys Rev E* 55:657
- 2518 139. Nelson DR (2002) *Defects and Geometry in Condensed Matter Physics*. Cambridge University Press, Cambridge
- 2519 140. Nicodemi M (1999) *Phys Rev Lett* 82:3734
- 2520 141. Pan AC, Garrahan JP, Chandler D (2005) *Phys Rev E* 72:041106
- 2521 142. Pardo LC, Lunkenheimer P, Loidl A (2007) *Phys Rev E* 76:030502(R)

- 2555 143. Parisi G, Zamponi F (2005) *J Chem Phys* 123:144501  
2556 144. Pusey PN and van Megen W (1986) *Nature* 320:340  
2557 145. Richert R, Angell CA (1998) *J Chem Phys* 108:9016  
2558 146. Ritort F, Sollich P (2003) *Adv Phys* 52:219  
2559 147. Rivoire O, Biroli G, Martin OC, Mézard M (2004) *Eur Phys J B*  
2560 37:55  
2561 148. Réfrégier P, Vincent E, Hammann J, Ocio M (1987) *J Phys*  
2562 France 48:1533  
2563 149. Sethna JP, Shore JD, Huang M (1991) *Phys Rev B* 44:4943  
2564 150. Sollich P, Lequeux F, Hebraud P, Cates ME (1997) *Phys Rev*  
2565 Lett 78:2020  
2566 151. Sollich P (1998) *Phys Rev E* 58:738  
2567 152. Struik LCE (1978) *Physical aging in amorphous polymers and*  
2568 *other materials*. Elsevier, Amsterdam  
2569 153. Szamel G, Flenner E (2004) *Europhys Lett* 67:779  
2570 154. Tarjus G, Kivelson D (1995) *J Chem Phys* 103:3071  
2571 155. Tarjus G, Kivelson SA, Nussinov Z, Viot P (2005) *J Phys Con-*  
2572 *dens Matter* 17:R1143  
2573 156. Thalmann F (2002) *J Chem Phys* 116:3378  
2574 157. Toninelli C, Biroli G, Fisher DS (2004) *Phys Rev Lett* 92:185504  
2575 158. Toninelli C, Biroli G, Fisher DS (2006) *Phys Rev Lett* 96:035702  
2576 159. Toninelli C, Wyart M, Berthier L, Biroli G, Bouchaud J-P (2005)  
2577 *Phys Rev E* 71:041505  
2578 160. Tracht U, Wilhelm M, Heuer A, Feng H, K Schmidt-Rohr,  
2579 Spiess HW (1998) *Phys Rev Lett* 81:2727 (Reinsberg SA, Qiu  
2580 XH, Wilhelm M, Spiess HW, Ediger MD (2001) *J Chem Phys*  
2581 114:7299) **TS4**  
2582 161. Vidal Russell E, Israeloff NE (2000) *Nature* 408:695  
2583 162. Viot P, Talbot J, Tarjus G (2003) *Fractals* 11:185  
2584 163. Vogel M, Glotzer SC (2004) *Phys Rev E* 70:061504  
2585 164. Wang P, Song CM, Makse HA (2006) *Nat Phys* 2:526  
2586 165. Weeks E, Crocker JC, Levitt AC, Schofield A, Weitz DA (2000)  
2587 *Science* 287:627  
2588 166. Weeks ER, Crocker JC, Weitz DA (2007) *J Phys Condens Matter*  
2589 19:205131  
2590 167. Whitelam S, Berthier L, Garrahan JP (2005) *Phys Rev E*  
2591 71:026128  
2592 168. Whitelam S, Berthier L, Garrahan JP (2004) *Phys Rev Lett*  
2593 92:185705  
2594 169. Whitelam S, Garrahan JP (2004) *J Phys Chem B* 108:6611  
2595 170. Wuttke J, Petry W, Pouget S (1996) *J Chem Phys* 105:5177  
2596 171. Xia XY, Wolynes PG (2000) *Proc Natl Acad Sci USA* 97:2990  
2597 172. Yamamoto R, Onuki A (1998) *Phys Rev E* 58:3515  
2598 173. Young AP (ed) (1998) *Spin glasses and random fields*. World  
2599 Scientific, Singapore

Uncorrected Proof  
2008-04-18